Suppressed Ion Chromatography of Organic Acids with Universal Detection

by

Naama Karu
(B.Sc, M.Sc)

A thesis submitted in fulfilment of the requirements for the degree of

Doctor of Philosophy

UNIVERSITY OF TASMANIA

School of Chemistry
University of Tasmania
Hobart

Submitted May 2012

DECLARATION

I hereby declare that this thesis contains no material which has been accepted for a degree or diploma by the University or any other institution, except by way of background information and duly acknowledged in the thesis, and to the best of the my knowledge and belief no material previously published or written by another person except where due acknowledgement is made in the text of the thesis, nor does the thesis contain any material that infringes copyright.

Naama Karu

The publishers of the papers comprising Chapters 4 to 7 hold the copyright for that content, and access to the material should be sought from the respective journals. The remaining non published content of the thesis may be made available for loan and limited copying and communication in accordance with the Copyright Act 1968.

Naama Karu

University of Tasmania

Hobart

May, 2012

STATEMENT OF CO-AUTHORSHIP

The following people and institutions contributed to the publication of the work undertaken as part of this thesis:

- Candidate: N. Karu, Pfizer Analytical Research centre (PARC), ACROSS, School of Chemistry, UTAS.
- G.W. Dicinoski, Pfizer Analytical Research centre (PARC), ACROSS, School of Chemistry, UTAS.
- P.R. Haddad, Pfizer Analytical Research centre (PARC), ACROSS, School of Chemistry, UTAS.
- J.P. Hutchinson, Pfizer Analytical Research centre (PARC), ACROSS, School of Chemistry, UTAS.
- M. Hanna-Brown, Analytical R&D, Pfizer Global R&D, UK.
- C.A. Pohl, R&D, Thermo Fisher Scientific, Sunnyvale, CA, USA.
- K. Srinivasan, R&D, Thermo Fisher Scientific, Sunnyvale, CA, USA.

Chapters 3 to 7 are based on 4 parts of a series of papers titled: "Determination of pharmaceutically related compounds by suppressed ion chromatography".

Details of the authors roles:

Papers [1] and [2], "I. Effects of organic solvent on suppressor performance"; "II. Interactions of analytes with the suppressor", located in chapters 4 and 5, respectively.

N. Karu (65%), G.W. Dicinoski (13%), M. Hanna-Brown (2%), P.R. Haddad (20%)

- N. Karu contributed to the design of the overall concept, experimental plan, executed all laboratory work and wrote the draft manuscript.
- G.W. Dicinoski and P.R. Haddad contributed to the idea, its formalisation and development.
- P.R. Haddad assisted with publication refinement and presentation.
- M. Hanna-Brown established the need of study and provided feedback on the work.

Paper [3], "III. Role of electrolytic suppressor design", located in chapter 6.

N. Karu (60%), G.W. Dicinoski (10%), M. Hanna-Brown (2%), C.A. Pohl (3%), K. Srinivasan (10%), P.R. Haddad (15%)

- N. Karu contributed to the design of the overall concept, experimental plan, executed all laboratory work and wrote the draft manuscript.
- K. Srinivasan provided the modified suppressors, supervised the laboratory work and provided valuable feedback.
- G.W. Dicinoski, P.R. Haddad, C.A. Pohl and K. Srinivasan contributed to the idea, its formalisation and development.
- P.R. Haddad and K. Srinivasan assisted with publication refinement and presentation.
- M. Hanna-Brown established the need of study.

Paper [4], "IV. Interfacing ion chromatography with universal detectors", located in chapter 7.

N. Karu (55%), J.P. Hutchinson (12%) G.W. Dicinoski (8%), M. Hanna-Brown (2%), C.A. Pohl (3%), K. Srinivasan (5%), P.R. Haddad (15%)

- N. Karu contributed to the design of the overall concept, experimental plan, executed all laboratory work, and wrote the draft manuscript.
- J.P. Hutchinson contributed to the experimental design and data analyses.
- K. Srinivasan provided the modified suppressor and gave valuable feedback.
- G.W. Dicinoski, P.R. Haddad, C.A. Pohl and K. Srinivasan contributed to the idea, its formalisation and development.
- P.R. Haddad G.W. Dicinoski and J.P. Hutchinson assisted with publication refinement and presentation.
- M. Hanna-Brown established the need of study.

We the undersigned agree with the above stated "proportion of work undertaken" for each of the above published (or submitted) peer-reviewed manuscripts contributing to this thesis:

Signed: _____ _____

Prof. Paul Haddad
Supervisor
School Of Chemistry
University of Tasmania

Prof. Emily Hilder
Post-Graduate Coordinator
School of Chemistry
University of Tasmania

Date: _____

ACKNOWLEDGEMENTS

This project was supported by a PhD Scholarship from PARC (Pfizer Analytical Research Center), ACROSS (Australian Center for Research on Separation Science), together with the University of Tasmania. The tuition fee was covered by a grant from the State Government of Tasmania, Department of Economic Development and Tourism. A travel grant to attend an overseas conference and research visit was kindly provided by the UTAS Graduate research office, the School of Chemistry, CASSS (International Chromatography society) and Dionex Corporation (Part of Thermo-Fisher Scientific).

I would like to express my gratitude to the following people:

- My supervisors Prof. Paul Haddad and Assoc. Prof. Greg Dicinoski for their support and advice during the course of this project.
- Dr. Phil Zakaria, Dr. Joseph Hutchinson, and Mr. Tim Causon for helpful discussions and for their kind assistance in proof-reading my work.
- Past and present members of ACROSS and PARC for their friendship, help and collaboration throughout the course of my PhD candidature, including Prof. Emily Hilder, Prof. Pavel Nesterenko, Assoc. Prof. Robert Shellie, Assoc. Prof. Michael Breadmore, Assoc. Prof. Lito Quirino, Dr. Cameron Johns, Dr. Anna Nordborg, Dr. Eadaoin Tyrrell, Dr. Dario Arrua, Dr. Tom Kazarian, Dr. Paul Harvey, Dr. Wei Boon (Jason) Hon, Dr. Oscar Potter, Mr. Yi Heng (Ryan) Nai, Ms. Esme Candish, Mr. Tomas Remenyi, Mr. Marc Guijt, Ms. Helen Barnard, Mr. Anthony Malone, Ms. Clodagh Moy.
- The staff and students of the School of Chemistry for providing such a friendly working environment.
- The staff members of ThermoFisher Scientific – Dionex, Sunnyvale, CA, USA for their support, friendship, advice and patience during my research visit (May-June 2011). Special thanks to Mr. Chris Pohl, Dr. Kannan Srinivasan, Ms. Sheetal Bhardwaj, Dr. Rahmat Ullah, Ms. Willy DeHaas, Ms. Maria Rey, Dr. Bill Schnute, Mr. Marcus Miller, Ms. Terri Christison, Mr. Jay Lorch, Ms. Alex Kirkland, Mr. Jesse Diaz.

LIST OF ABBREVIATIONS

AAES	Anion Atlas electrolytic suppressor
AAS	Atomic absorption spectroscopy
ACN	Acetonitrile
AES	Atomic emission spectroscopy
ANOVA	Analysis of variance
CAD	Charged aerosol detector
CD	Conductivity detector
CPC	Critical point concentration
CR-TC	Continuously regenerated trap column
EDTA	Ethylene-diamine-tetra-acetic acid
ELSD	Evaporative light-scattering detector
EPA	Environmental Protection Agency
ESI-MS	Electro-spray ionisation Mass spectrometry
HC	High capacity
HILIC	Hydrophilic-interaction liquid interface chromatography
HPAE	High-Performance anion exchange
HPLC	High-Performance liquid chromatography
HSA	Hexane-sulfonic acid
IC	Ion chromatography
ICP	Inductively coupled plasma
IE	Ion exchange
LOD	Limit of detection
LLOQ	Low limit of quantification
MeOH	Methanol
MMS	Micro-membrane suppressor
MNG; MENG	Micro-electrolytic NaOH generator
MSC	Maximum suppression capacity
NP	Normal-phase
NSAID	Non-steroidal anti inflammatory drug
PAA	Phenylacetic acid

LIST OF ABBREVIATIONS - CONTINUED

PCR	Post-column reaction
PTFE	poly(tetrafluoroethylene), Teflon®
PSA	Polar surface area
RPLC	Reversed-phase liquid chromatography
RSD	Relative standard deviation
S/N	Signal-to-noise ratio
SD	Standard deviation
SIM	Selected ion monitoring
SPE	Solid phase extraction
SPR	Solid phase reagent
SRS	Self-regenerating suppressor
UHPLC	Ultra-high pressure liquid chromatography

LIST OF PUBLICATIONS

Papers in refereed journals and in preparation

1. N. Karu, G.W. Dicinoski, M. Hanna-Brown, P.R. Haddad. Determination of pharmaceutically related compounds by suppressed ion chromatography: I. Effects of organic solvent on suppressor performance. *J. Chromatogr. A.* 1218 (2011) 9037. *(Chapter 4)*
2. N. Karu, G.W. Dicinoski, M. Hanna-Brown, P.R. Haddad. Determination of pharmaceutically related compounds by suppressed ion chromatography: II. Interactions of analytes with the suppressor. *J. Chromatogr. A.* 1224 (2012) 35. *(Chapter 5)*
3. N. Karu, G.W. Dicinoski, M. Hanna-Brown, K. Srinivasan, C.A. Pohl, P.R. Haddad. Determination of pharmaceutically related compounds by suppressed ion chromatography: III. Role of electrolytic suppressor design. *J. Chromatogr. A.* 1233 (2012) 71. *(Chapter 6)*
4. N. Karu, J.P. Hutchinson, G.W. Dicinoski, M. Hanna-Brown, P.R. Haddad. Determination of pharmaceutically related compounds by suppressed ion chromatography: IV. Interfacing ion chromatography with universal detectors. (*Submitted to J. Chromatogr. A*). *(Chapter 7)*

Presentations at international conferences (presenting author underlined)

1. N. Karu, G.W. Dicinoski, M. Hanna-Brown, P.R. Haddad. Analysis of pharmaceutically-related compounds by suppressed ion chromatography, Poster presentation, *11th Asia-Pacific International Symposium on Microscale Separations and Analysis (APCE),* 2011, Hobart, Australia.
2. P.R. Haddad, G.W. Dicinoski, N. Karu, V. Drgan, B. Ng, P. Zakaria, R.A. Shellie. Extending the Scope of Ion Chromatography, Oral presentation, *37th International symposium on High Performance Liquid Phase Separations and related techniques (HPLC)*, 2011, Dalian, China.
3. P. R. Haddad, G.W. Dicinoski, R.A. Shellie, B.K. Ng, E.F. Hilder, P.N. Nesterenko,

P. Zakaria, V. Drgan, N. Karu. Recent Advances in Ion Chromatography, Oral presentation, *36th International symposium on High Performance Liquid Phase Separations and related techniques (HPLC)*, 2011, Budapest, Hungary.

4. N. Karu, G.W. Dicinoski, M. Hanna-Brown, P.R. Haddad. Suppression of Ionic Eluents Containing Organic Solvents as a normalisation step before coupling to Universal Detectors: Performance and Limitations, Oral presentation, *35th International symposium on capillary chromatography (ISCC)*, 2011, San Diego, CA, USA.

5. N. Karu, G.W. Dicinoski, M. Hanna-Brown, P.R. Haddad. Expanding the Role of Ion Chromatography in Pharmaceutical analysis: Suppressed Universal Detection of Non-Chromophoric Compounds, Poster presentation,
   - *22nd International Ion Chromatography Symposium (IICS)*, 2010, Cincinnati, Ohio, USA.
   - *35th International Symposium on High-Performance Liquid Phase Separations and Related Techniques (HPLC)*, 2010, Boston, USA.

6. P.J. Zakaria, N. Karu, G.W. Dicinoski, M. Hanna-Brown, P.R. Haddad. Expanding the role of Ion Chromatography in Pharmaceutical analysis, Oral presentation, *34th International symposium on capillary chromatography (ISCC)*, 2010, Riva del Grada, Italy.

7. N. Karu, G.W. Dicinoski, M. Hanna-Brown, P.R. Haddad. Multiple Approaches for Non-Chromophoric Pharmaceutical Detection, Poster presentation, *34th International Symposium on High-Performance Liquid Phase Separations and Related Techniques (HPLC)*, 2009, Dresden, Germany. *(Chapter 3)*

8. N. Karu, G.W. Dicinoski, M. Hanna-Brown, P.R. Haddad. Conductivity Signal-Enhancement for the Detection of Organic Ions, Poster presentation, *ACROSS Symposium on Advances in Separation Science (ASASS),* 2008*,* Hobart, Australia. *(Chapter 3)*

ABSTRACT

This work presents an investigation into the challenges involving the utilisation of ion chromatography (IC) for the identification of impurities in pharmaceutical compounds, which is an essential task in the pharmaceutical industry.

In IC, the use of a suppressor results in insensitive conductivity responses when applied to weak acids. In an attempt to circumvent this problem, signal enhancement through a post-suppressor reaction was performed by introducing a low concentration of a basic reagent, via a tee-connector, into the suppressor effluent. This approach exhibited enhancements of up to 500-fold for weak acids with pK_a >4.7. However, signal enhancement was limited to high concentrations and sample volumes (at least 10 nmol on column), and did not greatly improve the limits of detection due to 50-100 times increase in baseline noise after reagent mixing. pH detection was also assessed, either after suppression or after base introduction, yet it hardly exhibited any signal enhancement of weak acids and at best resulted in limits of detection 4-times lower than suppressed conductivity.

Universal detection methods suitable for coupling to IC were then investigated. However, the non-volatile ionic eluents commonly used in IC pose an obstacle in coupling to mass spectrometry (MS) and aerosol-based detectors, as the high ionic content can cause severe interferences in these detectors. A detailed study of the use of commercially-available chemical or electrolytic suppressors for desalting eluents comprising isocratic or gradient steps and containing organic solvents was undertaken.

First, chemical and electrolytic suppressors were evaluated for baseline drift, noise and efficiency of suppression using aqueous/organic eluents containing up to 40% (v/v) methanol or acetonitrile. Chemical suppression of aqueous/organic eluents showed minimal noise levels, uniform low baseline and low gradient drift. Electrolytic suppression gave good performance, but with higher baseline conductivity levels and baseline drift than chemical suppression. The elevated baseline was found not to be caused by incomplete suppression of the eluent, but was attributed to chemical reactions involving the organic solvents and facilitated by high electric currents and heat generation. It was demonstrated that suppressed ion-exchange separation using a complex KOH elution profile could be coupled with an evaporative light-scattering

detector (ELSD), with the suppressor effectively de-salting the eluent, producing a stable baseline.

Second, the interactions between the suppressor and weak organic acid analytes, including pharmaceutically-related compounds, were investigated for eluents containing organic solvents. Correlations were observed between analyte recovery rates after electrolytic suppression and the eluent composition, the suppression conditions, and the physico-chemical properties of the analytes. These results suggest that hydrophobic adsorption interactions occur in the electrolytic suppressor and that these interactions are ameliorated by the addition to the eluent of high levels of organic solvents, especially acetonitrile, leading to 5-15% analyte losses. Use of eluents containing 80% acetonitrile resulted in very low losses of analyte during suppression (1-8%). Recovery experiments conducted in various compartments of the electrolytic suppressor showed that some analytes permeated through the suppressor membrane into the regenerant chambers, but this could be prevented by adding organic solvent to the regenerant solution. It was also noted that analyte losses increased with aging of the electrolytic suppressors, to levels of 15-35% loss. Chemical suppression avoids some of the analyte losses observed with an electrolytic suppressor, but when used under the correct conditions, electrolytic suppressors gave close to equivalent performance to chemical suppressors.

Following the above studies, three new prototype designs for the electrolytic suppressors comprising high ion-exchange capacity screens and membranes were developed. These designs aim to minimise hydrophobic interactions of the suppressor with organic analytes and to provide higher compatibility with eluents containing acetonitrile. In comparison with a commercially-available electrolytic suppressor and also a commercially-available chemical suppressor, the new high-capacity suppressor showed superior performance, exhibiting minimal interactions with a test set of analytes under the examined conditions. This led to the attainment of high recoveries of the analytes after suppression (93-99% recovery) and significantly reduced band broadening during suppression. The new suppressor has been shown to perform well under both isocratic or gradient elution conditions.

For proof of concept, IC was coupled to an electro-spray-ionisation mass spectrometer (ESI-MS), a corona charged aerosol detector (CAD), an evaporative

light-scattering detector (ELSD), and a UV detector, which served as a reference detection technique. Suppression of the ionic gradient containing moderate concentrations of organic solvent was conducted by employing the new electrolytic suppressor design, and compared to a chemical suppressor. Complex elution profiles could be applied for separation, without the complications of organic solvent gradients typical to reversed-phase (RP) HPLC. The limits of detection were not greatly compromised by the suppressed system, yielding values of low ng/mL with MS detection, low to sub-µg/mL levels with the CAD and 2-20 µg/mL with the ELSD. When coupled to MS, CAD and UV detectors, the modified electrolytic suppressor showed precision in peak areas of 0.4%-2.5%, outperforming to the chemical suppressor which yielded averages of 1.5-3 fold higher %RSDs. The modified electrolytic suppressor also generally exhibited wider linear response ranges than the chemical suppressor. Most importantly, complementary selectivity to reversed-phase separation was demonstrated for the test analytes as well as sample impurities, showcasing the use of IC as an orthogonal separation technique in the pharmaceutical industry.

TABLE OF CONTENTS

Page

Chapter 1

Introduction and Literature Review

1.1. Introduction

Ion chromatography (IC) is a well established separation technique which is based on the different distribution of ionic analytes between the oppositely-charged stationary phase ("column") and the ionic mobile phase ("eluent") which is commonly a dilute solution of acid, base or salt [1]. IC is applied extensively for the analysis of water and in the environmental and food industries, as detailed in reviews [2,3] and books [1,4]. Various government and regulatory organisations, such as the United States Environmental Protection Agency (EPA) [5] employ IC in regulatory methods.

Chemical analysis in the pharmaceutical industry is conducted mainly using reversed-phase (RP) and normal-phase (NP) high-performance liquid chromatography (HPLC), and atomic spectroscopic techniques, such as atomic absorption spectroscopy (AAS) and inductively coupled plasma atomic emission spectroscopy (ICP-AES) [6]. For the analysis of ionic and ionogenic pharmaceuticals, IC offers a complementary method to RPLC due to the difference in separation mechanism. IC has been utilised in the pharmaceutical industry primarily for the analysis of inorganic ionic compounds or counter-ions of charged organic compounds [1,6], and when coupled with conductivity detection, it has offered a useful separation method for these analytes.

In contrast to the majority of pharmaceutically-related inorganic ions analysed by IC, the target analytes in this study are active pharmaceutical ingredients (or their surrogates) which are weak or very weak organic acids. Therefore, if IC is to be used for their analysis, an investigation is required to assess the compatibility of the existing methods and instrumentation and to determine the extent of adaptation necessary in operational and detection aspects.

1.2. Ion Chromatography

1.2.1. Background

IC is a term used to describe a number of liquid chromatography techniques, including ion-exchange chromatography, ion-exclusion and ion-interaction chromatography (also termed ion-pairing chromatography). The target analytes of these methods are traditionally inorganic anions and cations and low-molecular weight organic acids and bases [1,4,7]. In recent years the utilisation of IC has expanded to the analysis of additional analyte groups [7-11], such as carbohydrates, amino acids, nucleic acids and proteins [12-15]. The common detection methods in IC are conductivity (suppressed or non-suppressed), electrochemistry (amperometry and potentiometry) and spectrophotometry (direct or indirect) [1,4,16]. Post-column reactions for signal enhancement are also employed with this technique [17-19].

1.2.2. Ion-exclusion chromatography

Since ion-exclusion is referenced later in this review, it is briefly discussed here. In 1953, Wheaton and Bauman reported the separation of weak anions from strong acids by ion-exclusion [20], explained by the Donnan exclusion effect on the strong ion-exchange stationary phase [21]. While charged analytes having the same charge as the ionic stationary phase are repelled from the ionic resin and eluted quickly, weakly ionised and non-ionic species can penetrate into the occluded liquid phase and are retained. The suitable stationary phase would be, for example when separating weak carboxylic acids, cation-exchange resin with sulfonated functional groups [1]. Both suppressed and non-suppressed conductivity detection have been applied after ion-exclusion. However, when dilute strong acids are required in the eluent for separation, then direct conductivity detection is not feasible [7], and signal enhancement via indirect detection can be performed.

1.2.3. Principles of Ion-exchange chromatography

Ion-exchange is a variant of IC that employs columns filled with resin material (polymeric or inorganic) with fixed charged groups on its surface [1]. Anion-exchange columns contain resin with positively-charged groups, while cation-exchange columns contain resin with negatively-charged groups. The application of an eluent with ions of

the opposite charge maintains electrical neutrality. The ion-exchange process is illustrated by an anion-exchange system, which is the form of IC employed as the key separation mode in this work. Commercially-available anion-exchange columns are more diverse than cation-exchange columns and are also compatible with organic solvents. When a negatively-charged analyte (A^-) is injected onto the column, it binds to the positively-charged resin (R^+) via electrostatic interactions, replacing an equivalent number of eluent anions (E^-) which were attached originally to the sites. This anion-exchange process is an equilibrium, as detailed in Equation 1.1 (adapted from [1]):

$$Resin \cdots R^+E^- + A^- \rightleftarrows Resin \cdots R^+A^- + E^- \quad (1.1)$$

The analyte anion A^- can be eluted from the resin by applying a higher concentration or a stronger competing anion (E^-) in the eluent, such as a dilute solution of KOH. The equilibrium constant for this process is defined as the selectivity coefficient for the column, which can be generalised to include polyvalent ions, and expressed as Equation 1.2:

$$K_{(A,E)} = \frac{\left(A_R^{x-}\right)^y \cdot \left(E_M^{y-}\right)^x}{\left(A_M^{x-}\right)^y \cdot \left(E_R^{y-}\right)^x} \quad (1.2)$$

where *A* (analyte anion) or *E* (eluent anion) can be either in the mobile phase (*M*) or on the column resin (*R*); *x* is the charge on *A* and *y* is the charge on *E*; The parentheses indicate the activity of each species.

Analytes with different selectivity coefficients for a specific combination of resin and eluent anion will be separated due to different degrees of interaction with the stationary phase, which dictate their retention times. The mechanism for cation-exchange separation is analogous. This work has concentrated on post-column reactions and detection rather than the separation of analytes, therefore the separation aspects are not widely discussed in the review.

1.2.4. Conductivity detection

Electrical conductivity measures the ability of a solution to conduct an electric current between two electrodes across which an electric field has been applied. The conductance of a solution (*G*) is commonly expressed by the SI unit Siemens (S), and is the reciprocal of the resistance (*R*) to the electric current measuring ohms (Ω) [7]:

$$G = \frac{1}{R} \tag{1.3}$$

Conductivity detectors are simple devices consisting of a detection cell with two electrodes, which can either be in contact with the stream of electrolyte (standard detector) or not (contactless conductivity detector) [7]. Conductivity detection is the natural choice for IC, since the separated analytes are electrically conducting, making conductivity practically a universal detection option [16,22]. The conductance is affected by temperature, yet the conductivity detectors applied in IC systems are temperature-controlled and compensate electronically according to the temperature requirements.

The conductance signal depends on the electrolyte concentration (*C*) of the ionic species present (both eluent and analyte ions, *either + or* -) and their limiting equivalent ionic conductances (λ), which are readily available in literature for common anions and cations [1,7,19]. For anion-exchange, used here for illustrating the operating principles, the background conductance (*G*, in units of µS) of the eluent (*E*) would be given by Equation 1.4 [19]:

$$G_{Background} = \frac{(\lambda_{E^+} + \lambda_{E^-}) \cdot C_E}{10^{-3} \cdot K} \tag{1.4}$$

where *K* [cm^{-1}] is the conductivity detector cell constant expressing the ratio of the distance between the electrodes (in cm) and the area of the electrodes (in cm^2). Since this value slightly differs even between identical instruments, *K* is determined for each conductivity cell by a standard calibration procedure. The baseline conductance *G* of an eluent consisting of a fully dissociated salt (such as 1 mM potassium chloride) is recorded, and then corrected to give the expected specific conductance *k* (according to Equation 1.4 without *K*), by multiplying *G* by *K*.

In the case of a fully-dissociated analyte (*A*), the conductance of the eluting analyte band is given by Equation 1.5 (adapted from [19]):

$$G_{Elution} = \frac{(\lambda_{E^+} + \lambda_{E^-}) \cdot C_E + (\lambda_{A^-} - \lambda_{E^-}) \cdot C_A}{10^{-3} \cdot K} \tag{1.5}$$

The change in conductance accompanying elution of the analyte is therefore given by Equation 1.6 [19]:

$$\Delta G_{(Elution\ -Background\ )} = \frac{(\lambda_{A^-} - \lambda_{E^-})\cdot C_A}{10^{-3}\cdot K} \quad (1.6)$$

If both the analyte and the eluent are only partly ionised at the pH of the eluent, the change in conductance upon elution of the analyte will follow Equation 1.7 (adapted from [19]):

$$\Delta G_{(Elution\ -Background\ )} = \left(\frac{(\lambda_{E^+} + \lambda_{A^-})\cdot\alpha_A - (\lambda_{E^+} + \lambda_{E^-})\cdot\alpha_E\cdot\alpha_A}{10^{-3}\cdot K}\right)\cdot C_A \quad (1.7)$$

where α is the fraction of the species (*A* or *E*) which is dissociated. It can be observed that if full ionisation has occurred for both the eluent and the analyte ($\alpha_E = \alpha_A = 1$) then Equation 1.7 is simplified to give Equation 1.6. According to Equation 1.7, the higher the ionisation of the analyte (α_A), the higher the conductance signal. In a non-suppressed eluent system, lower ionisation of the eluent (α_E) is desirable since it leads to higher total conductance signal. For that reason partly-ionised eluents such as benzoate and phthalate have been employed in this method [23,24]. When non-dissociated eluents are used, they can contribute hydronium to the analyte band, resulting in enhancement of the conductivity signal, similarly to the effect achieved in suppressed conductivity [19].

1.3. Suppressed conductivity

1.3.1. Principles

Suppression is a post-column reaction which results in decreased background conductivity. The suppression reaction implemented in the IC system is usually of an acid-base nature, involving stoichiometric neutralisation of ionic eluent and elimination of the analyte counter-ion [22].

For an anion separation system, the primary mode utilised in this work, hydroxide eluents are advantageous since they form water upon suppression. Considering this case, the reaction in the suppressor will follow Equation 1.8 (adapted from [19]):

$$Resin\cdots H^+ + K^+OH^- \rightleftarrows Resin\cdots K^+ + H_2O \quad (1.8)$$

This exchange process results in an enhanced signal-to-noise ratio, achieved by the decrease in the background conductance from the value calculated by Equation 1.3 to a

level close to 0 µS, if full suppression has occurred. A stoichiometric ion-replacement is critical for gaining repeatable and sensitive conductivity response, since remnants of eluent counter-ions elevate the baseline and directly affect the limits of detection (LOD).

The reaction of an analyte anion (A^-) in the suppressor will follow Equation 1.9:

$$Resin\cdots H^+ + K^+A^- \rightleftarrows Resin\cdots K^+ + H^+ + A^- \quad (1.9)$$

This effect is accompanied by an increase in the analyte conductance due to the higher limiting equivalent ionic conductance of H^+ compared to the original analyte counter-ion K^+ [19].The increase in conductance after suppression, however, depends on the degree of ionisation of the analyte at the pH of the suppressed eluent, given by the acid dissociation constant K_a and its logarithmic form pK_a:

$$pK_a = -log\left(\frac{[H^+]\cdot[A^-]}{[HA]}\right) \quad (1.10)$$

If the analyte pK_a is more than 1 unit higher than the pH of the solution, the analyte will be mostly protonated and thus poorly conducting. This problem with weakly ionised analytes is discussed thoroughly later in this chapter.

Taking into consideration the concentration of the ionised analyte after suppression, and any eluent components which have not been neutralised into water, the conductance of an eluting analyte (*A*) is given by Equation 1.11:

$$G_{Analyte} = \frac{(\lambda_{H^+}\cdot[\mathrm{H^+}] + \lambda_{OH^-}\cdot[\mathrm{OH^-}] + \lambda_{K^+}\cdot[\mathrm{K^+}] + \lambda_{A^-}\cdot[\mathrm{A^-}])}{10^{-3}\cdot K} \quad (1.11)$$

If quantitative acid-base reaction has occurred and the analyte is fully dissociated at the pH of the suppressed eluent, the detector signal of the analyte band will be given by the simplified Equation 1.12:

$$G_{Analyte} = \frac{(\lambda_{H^+} + \lambda_{A^-})\cdot C_A}{10^{-3}\cdot K} \quad (1.12)$$

1.3.2. Evolution of suppression methods and devices

IC with chemical suppression was introduced in 1975 by Small *et al*. who used an ion-exchange resin packed in a “stripper” column [25], implementing the principles detailed in the previous section. Suppressed conductivity, patented by the Dow Chemical company and licensed to the company which later became “Dionex”, was

mainly used for inorganic ions [26]. The major limitation of the packed-bed suppressors was the requirement for periodic off-line regeneration with a stream of strong electrolyte once its capacity had been exhausted. In addition, the high-capacity resin retained weaker solute ions, causing poor repeatability of peak heights [17], and also band broadening leading to a reduction in separation efficiency. Nevertheless, the performance of the packed-bed suppressors satisfied the market requirements at the time and hindered the development of previously-examined prototypes for membrane suppressors [27].

The first continuously-regenerated membrane suppressors were developed, independently in two laboratories, at the beginning of the 1980s, and were made of polymeric ion-exchange membranes in tubing or bundled hollow-fibres [28,29]. In Stevens' patented hollow fibre suppressor, the eluent flow was through the lumen of the fibre, while a constant stream of regenerant solution (containing the required ions for suppression) flowed counter-current along the exterior of the fibre. Although the fibre suppressor solved most of the shortcoming of the packed-bed suppressors, it had some disadvantages of its own. Limited by its design, the small internal diameter of the fibre meant low surface area for the suppression exchange, which translated into low suppression capacity [19]. This factor restricted the range of eluents and concentrations that could be used, not to mention the fact that steep gradient elution profiles could not be suppressed due to a drifting conductivity baseline. Other disadvantages of the hollow-fibre suppressors were the incompatibility with organic solvents, penetration of the regenerant into the eluent stream and also the inability to withstand high back-pressures from detectors positioned downstream [17]. The band broadening during suppression was greater than in packed-bed suppressors, which offset the improved peak shape obtained on newly-developed IC separation columns [27]. Subsequent development saw the band broadening reduced 4-fold owing to inert beads packed into the eluent side of the membrane, increasing the ion transport [30]. This packed-membrane suppressor also contained one length of Nafion ion-exchange tubing instead of a bundle of smaller sulfonated polyethylene hollow-fibres.

In 1985 the micromembrane suppressor ("MMS") was introduced by Dionex Corporation, incorporating flat-sheet ion-exchange membranes [22,31]. The micromembrane suppressor combined the advantages of the two previous techniques,

namely the high ion-exchange capacity of the packed-bed suppressors and continuous regeneration of the hollow-fibre suppressors. Its design, detailed in the next section, included minimal void volume of the suppressor flow path, which minimised the peak dispersion and improved the sensitivity, although it was also more prone to blocking [17]. The MMS provided a stable conductivity baseline with good, but not always complete suppression, resulting in background levels of ≤30 µS (equivalent to ~100 µM KOH). The MMS could suppress stronger eluents than the previous suppression methods (up to 10-fold higher concentrations), and it was compatible with organic solvents. The suppression of strong eluents in the gradient mode was an important ability of the MMS, since both suppressed and non-suppressed conductivity detection after gradient elution has previously been limited to certain eluents [32]. The extended choice of eluents that the membrane suppressors brought to the field enabled faster and more efficient separations with superior resolution, resulting in better peak shape and limits of detection. The shift to the suppressible carbonate and hydroxide-based eluents for anion separation also accelerated the development of columns and expanded the applicability of IC [33].

Suppressor leakage at high back-pressures was indicated as a problem of the MMS [17], though it was the consumption of large volumes of regenerant (up to 10 mL/min) that was the major disadvantage of the membrane suppressors. This problem was circumvented later on by a rather complex method of recycling the regenerant through a cartridge that converted the regenerant back to its initial form [34].

The limitations associated with the reliance on a constant chemical regenerant supply were further addressed in the late 1980s, with new designs of the membrane suppressor which incorporated electrodes. Electrochemical suppression was first demonstrated by Tian *et al.*, with an electric current applied across a flat-sheet membrane suppressor to enhance the mobility of ions compared to passive diffusion [35]. Full electrolytic suppression capability using solely hydrolysis of water to produce the replacement ions, was introduced by Strong and Dasgupta with the support of Dionex, using laboratory-made tubular membrane suppressors [36,37]. An electrolytic "self-regenerating suppressor" (SRS) became commercially-available through the Dionex Corporation in 1992 [38], with platinum electrodes being added to the basic structure of

the chemical micromembrane suppressor, as detailed in the next section along with its operation principles. An advanced feature of the electrolytic suppressor was its ability to consume the system effluent as a regenerant (termed "recycle mode") instead of using a constant supply of fresh water, although this approach was applicable only with aqueous eluents. When organic solvents are added to the eluent, they easily permeate through the suppressor membranes into the regenerant chambers, where they form oxidation by-products due to the electrolysis reaction [19,39]. These unwanted side-reactions can cause elevated conductivity baselines and increased noise levels, as discussed thoroughly in Chapter 4. Therefore, when the eluent contains organic solvents (up to 40% v/v) the source of water used as regenerant should be from an external source, and the application of higher regenerant flow-rate can be used to sweep out any baseline-elevating products. For the application of solvent content above 40% v/v in the eluent, it is recommended that the electrolytic suppressor is operated in full chemical suppression mode (without the application of the electric current) [38,40].

Despite the progress made in suppression technology and separation media [33], IC methods were still compromised by impurities in off-line prepared ionic eluents, mainly carbonate in hydroxide eluents introduced through adsorption of carbon dioxide from the air [10,41]. A few approaches for the production of purified ionic eluents were investigated by several researchers, utilising electrolysis reactions on ion-exchange media [37,42-44]. In 1997 Dionex Corporation released the electrolytic on-line eluent-generator, EluGen®, which automatically produced high-purity eluent from a reservoir of concentrated methanesulfonate (for cation separations) or potassium hydroxide (for anion separations), using deionised water as a carrier stream, in both isocratic or gradient modes [41,45]. The Dionex eluent generator was incorporated into a fully automated integrated high-performance IC system [26] which utilised rugged inert PEEK (polyetheretherketone) tubing and components instead of Tefzel tubing and metallic components [46]. The EluGen® was followed by a packed column suppressor for trapping carbonate contamination (named "CR-TC®", continuously regenerated trap column) [19,41]. The CR-TC utilises electrodialysis for maintaining the required charge form on its ion-exchange resin. At the same time, ionic contaminants from the eluent stream are driven towards the electrode with the opposite charge, where they react with the generated species and are quickly swept out of the CR-TC by another stream,

ideally the suppressor effluent [41]. Apart from ion-exchange, these electrolytic eluent generation and suppression devices have been employed in ion-exclusion methods, achieving higher sensitivity and better limits of detection [47].

The most recent electrolytic suppressor type developed by Dionex Corp. is the monolithic-based "Atlas®" electrolytic suppressor (AES) device, released in 2001 [48]. It combined the benefits of the previous suppressors: the low baseline noise levels gained by the MMS suppressor and the convenient electrolytic suppression of the SRS [49]. However, its suppression capacity is lower, it is aimed at carbonate-based eluents, and most importantly for this work, is not compatible with organic solvents. When compared to a low void volume 2 mm ASRS® (Anion SRS) which was modified to withstand higher flow-rate, the peak broadening caused by suppression was much higher on the AAES (Anion AES), leading to up to 10-fold lower peak efficiency of inorganic anions [50].

Since the expiration of the patent on the ion-exchange conductometric suppressor, alternative non-membrane suppressors were developed by companies other than Dionex Corp. [19]. These include different solid-phase suppressors, ranging from cheap but rugged disposable cartridges [51] to alternating systems [52] and continuously-generated column suppressors which are incorporated into the IC systems of Alltech [53,54] and Metrohm [55]. The new column suppressors have lower dead volume than the membrane suppressors, hence cause less band broadening. They can also withstand higher back pressure and flow-rates than the membrane suppressors [26]. Non-Dionex IC systems and solid-phase suppressors, despite being proven successful for various applications, are not in the scope of this work and will not be further discussed.

A few attempts have been made to combine an electrolytic suppressor with a conductivity detector [56,57]. The motivation behind this hybridisation was the reduced complexity with fewer system components, and lower dispersion which improves resolution and sensitivity [7]. The main obstacle to full integration of a conductivity detector with the commercially-available electrolytic suppressor is the immense difference in the applied current, with the suppressor operating in the range of 10-500 mA constant current [19,40,41], while a conductivity detector requires a supply at the µA level, and preferably an alternating current [7]. Huang *et al.* connected a continuously-regenerated packed column suppressor through a short inner-channel to a

resistance detector, using two independent current sources [57]. Common inorganic anions were separated by a sodium carbonate/bicarbonate eluent, suppressed by H^+ generated at the anode, and the analytes H^+X^- were detected as negative peaks on the baseline of HCO_3^- due to the decrease in the solution resistance. With the integrated suppressor-detector, the limits of detection were no better than 50% of the values measured with the standard combination of Dionex ASRS suppressor with a conductivity detector.

A rather unusual approach for eluent suppression was introduced by Gjerde and Benson in 1990, based on a post-column addition of a "solid phase reagent" ("SPR") without the body of a suppressor [58]. The reagent comprised a high-capacity ion-exchange resin with very small particles, which was introduced as a suspension via a tee connector to the column effluent, flowing towards the conductivity detector. The colloidal suspension, with conductivity of less than 10 µS, reacted with the eluent stream to produce a low-conductivity baseline. It removed any eluent counter-ion into the suspension, while at the same time converting sample ions to highly conducting species. The method was successfully applied for suppressed conductivity detection of a variety of analytes and eluents, in both isocratic or gradient modes [59,60]. Nevertheless, it was not established in the field due to disadvantages such as relatively high baseline noise and the expenses involved with resin consumption.

1.3.3. Micromembrane suppressors

1.3.3.1. Structure and mechanism

The membrane suppressor consists of a sandwich of flat ion-exchange membranes which separate a central eluent chamber from the regenerant chambers (Figure 1.1). The volume of the central eluent chamber is minimised (<50 µL), to reduce as much as possible the analyte band dispersion in the suppressor [22,61]. The regenerant solution flows into the suppressor through the regen-in port, where it is split to the two regenerant chambers and continues, flowing counter-current to the eluent, towards the regen-out port to waste. The counter-current flow ensures the availability of the regenerant ions at the membrane zone across from the eluent-in port [41]. The central channel, carrying the column effluent which entered through the eluent-in port, is independent of the flow in the regenerant channels.

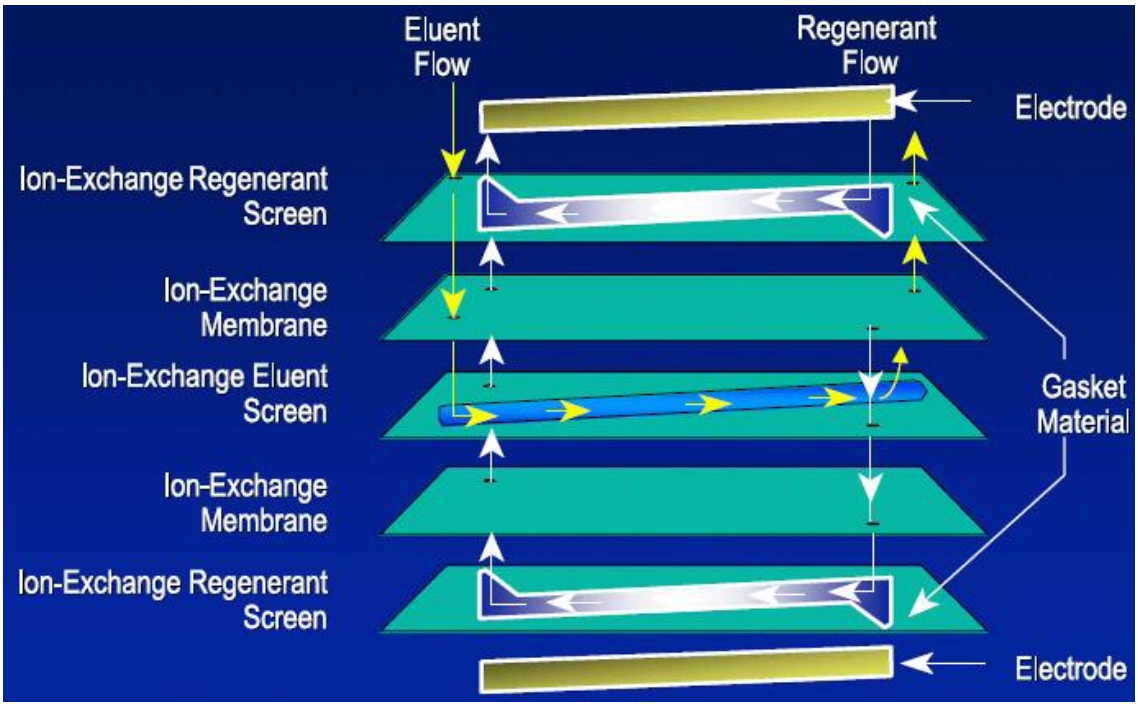

Figure 1.1 Membrane and screen configuration of the micromembrane suppressor, incorporating electrodes as appear in the electrolytic micromembrane suppressor. (extracted from ref. [41]).

The membranes are designed to allow permeation of ions of the same charge of its exchangeable ions while the permeation of ions of opposite charge (the analytes) is prohibited due to the Donnan exclusion effect of the charged membranes [61]. The membranes are made of polyethylene substrates, such as poly(tetrafluoroethylene) (PTFE, Teflon®), which is resistant to organic solvents and a wide range of pH. The substrates are first grafted with a suitable monomer (styrene and alkylstyrenes), for later functionalising. For example, a cation-exchange membrane is prepared by grafting the membrane sheets with styrene monomers, followed by functionalisation with sulfuric or sulfonic acids. The preparation of anion-exchange membrane involves modification by grafting with vinylbenzylchloride monomers, followed by functionalisation with alkyl tertiary amines (such as trimethylamine) or tertiary alkanolamines (such as dimethylethanolamine). The thickness of the membrane also plays a role in the mechanism of action, and for effective mass transport the thickness should preferably not exceed 25 µm.

The chambers contain charged screens, which may be formed from the same base polymers grafted with the same functionalised monomers as the membranes. The

use of ion-exchange screens improves both dynamic suppression capacity and chromatographic efficiency. The dynamic capacity of the suppressor is the concentration of eluent that can be suppressed per unit time. The screens in the regenerant chambers are functionalised to relatively high ion-exchange capacity, to serve as a reservoir for replacement ion from the regenerant. The screens also provide a site-to-site transfer path for the exchangeable ions, and owing to modified texture or weaving patterns, the screens interrupt laminar flow, thus enhancing mass transport to the membranes [61]. The mesh size of the screens should be relatively small to maintain chromatographic efficiency, yet not too small to hinder the liquid flow.

1.3.3.2. Chemical suppression

Chemical suppressors rely on a titration reaction of the eluent, and the parameters controlling chemical suppression are regenerant concentration and flow-rate, in proportion to those of the eluent. For anion suppression using the Dionex AMMS-300® described here (Fig. 1.2), the regenerant is dilute sulfuric acid, supplying hydronium ions to replace the counter-ion in the hydroxide-base eluent.

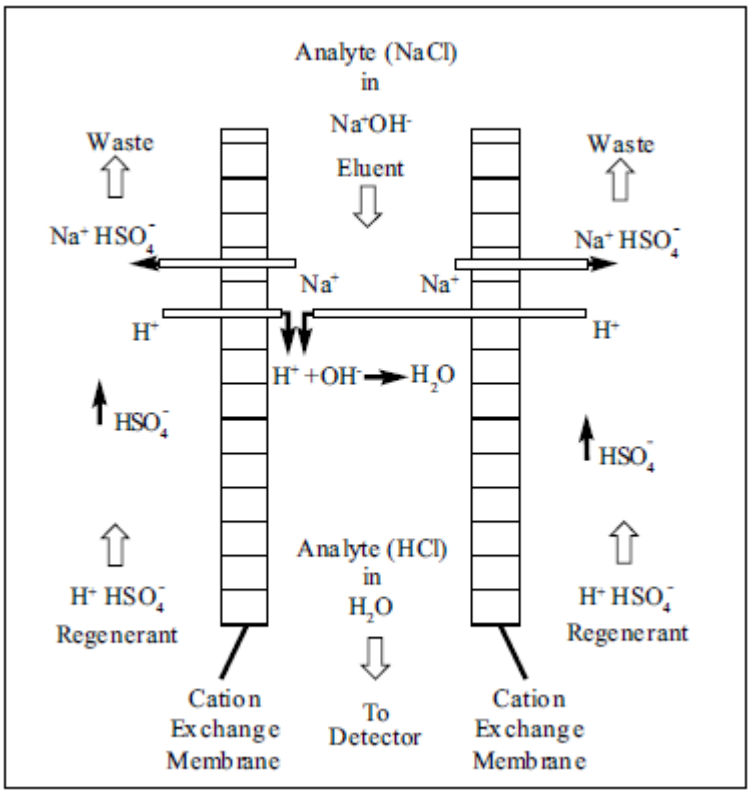

Figure 1.2 Chemical suppression mechanism by the anion micromembrane suppressor AMMS (extracted from ref. [62]).

The operational range is 1-100 mM mono-hydroxide eluent at a flow-rate of 0.5-1.5 mL/min, suppressed by sulfuric acid regenerant at a concentration of 50–100 mN (25-50 mM) applied at a flow-rate of 3-10 mL/min [62]. Once the regenerant concentration has been chosen, the regenerant flow-rate (mL/min) can be calculated based on the ratio between the dynamic concentration (mN·mL/min) of the regenerant and the eluent (Equation 1.13 [62]):

$$Regenerant\ flow = \frac{7 \cdot [eluent\ concentration\ (mN)] \cdot [eluent\ flow\text{-}rate\ (mL/min)]}{regenerant\ concentration\ (\mathrm{mN})} \quad (1.13)$$

The calculated values are defined as a starting point for choosing the regenerant flow-rate, optimised by monitoring the suppressor performance.

1.3.3.3. Electrolytic suppression

In electrolytic suppression, the source of hydronium ions (for anionic eluent suppression) and hydroxide (for cationic eluent suppression) is electrolysis of the water regenerant. As Figure 1.1 illustrates, two flat plate platinum electrodes are placed on the exterior sides of the gaskets defining the regenerant chambers, extending substantially across the length and width of the chambers in the gaskets [34]. The splitting of water molecules occurs when an electrical potential above ~1.5 V is applied across the electrodes, following Equation 1.14 at the anode and Equation 1.15 at the cathode [41], as also described in Figure 1.3.

$$H_2O \rightarrow 2H^+ + \tfrac{1}{2}\, O_2 + 2e^- \quad (1.14)$$

$$2H_2O + 2e^- \rightarrow 2OH^- + H_2 \quad (1.15)$$

The transfer of generated hydronium ions from the anode on the regenerant channel through the membrane into the eluent channel promotes the continuous regeneration to hydronium form. In the electrolytic suppressor, the replacement of eluent counter-ions occurs only on one of the membranes and not on two of them as in chemical suppression. Since this project requires eluents containing organic solvent, the electrolytic suppressor ASRS had to be operated under "AutoSuppression®" mode with external water supply, which is the only full electrolytic mode compatible with organic solvents, yet limited to 40% v/v solvent [40].

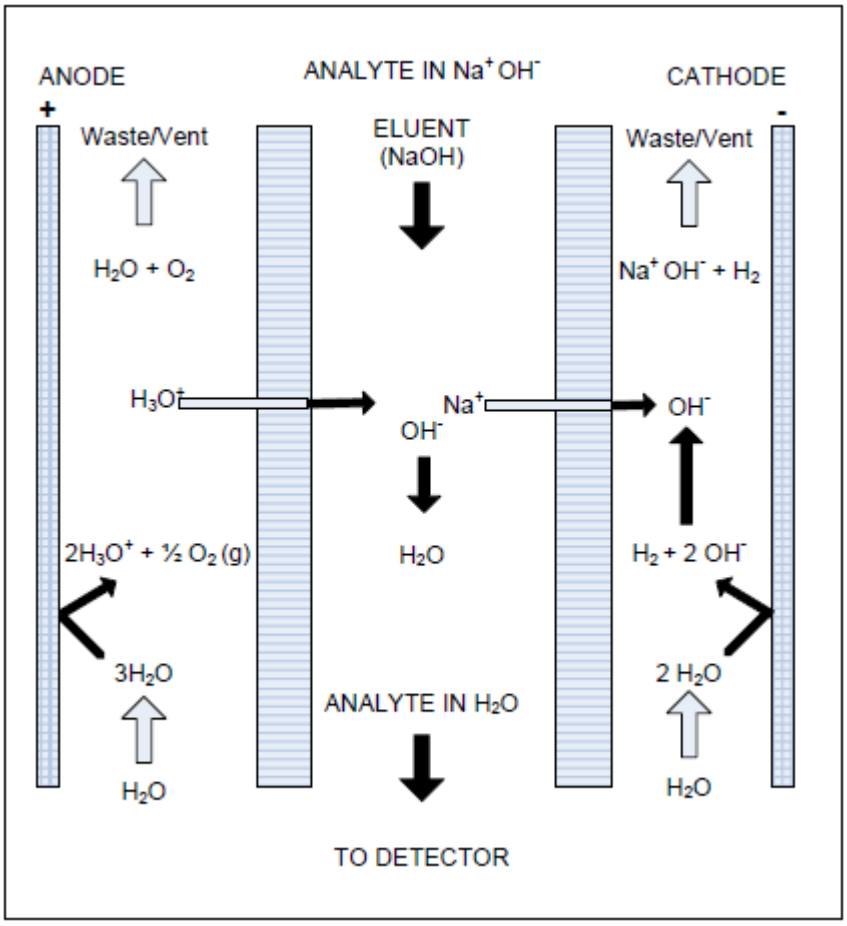

Figure 1.3 Electrolytic suppression mechanism by the anion self-regenerating suppressor ASRS (extracted from ref. [40]).

The key parameter controlling the extent of suppression in this mode is the level of applied current. With the water regenerant flow-rate playing only a minor role, it leaves a rather narrow operational space. The water regenerant flow-rate is independent of any equation, and should be kept in a range of 3-5 mL/min, with higher flow-rate used in the presence of high concentrations of organic solvent [39]. The optimal current is calculated according to Equation 1.16 [40]:

$$Current\ (mA) = 2.47 \cdot [Flow\ rate\ (mL/min)] \cdot [Eluent\ concentration\ (mN)] \quad (1.16)$$

The maximum suppression capacity (MSC) of the 4mm ASRS-300 is 200 µequiv., and its relation to other parameters is described in Equation 1.17 [40]:

$$MSC\ (mN \cdot mL/min) = [Flow\ rate\ (mL/min)] \cdot [Eluent\ concentration\ (mN)] \quad (1.17)$$

The modern electrolytic suppressors operate at 80-90% Faradaic efficiency [41]. The suppressor current is maintained at a constant value during separation to avoid fluctuations in the baseline [40]. Employing higher current on the ASRS (currents 10% above the ideal level) is not optimal, yet is required when a steep gradient is applied and the current is set to match the highest eluent concentration employed during the gradient run. At excessive current levels, higher amount of waste gas (hydrogen and oxygen) are produced at the electrodes and permeate through the membranes into the eluent channel. This then directly contributes to noise levels in the detector, especially when sufficient backpressure is not applied after the conductivity cell [40]. Also, the lifetime of the suppressor will be reduced under such condition due to high voltages and temperatures in the suppressor [38,63], which can also lead to loss of amphoteric analytes [64]. Although not recommended by the manufacturer, switching the suppressor current off for a limited period of time during a run was reported to significantly reduce background noise [65]. These aspects of operation are discussed in Chapters 4-6.

A comparison between the MMS and SRS and some considerations involved in choosing a suppression method in this work, are summarised in Table 1.1.

1.4. Conductivity signal enhancement by post-column reaction (PCR)

1.4.1. Early utilisation

The original purpose of post-suppression devices in IC was to confront the frequent problems of eluent impurities and inefficient suppression, by lowering the background conductivity. For example, gas permeable PTFE tubing was used as a post-suppressor to eliminate undesired carbonic acid in a suppressed carbonate eluent. The permeation of carbon dioxide through the porous tubing dramatically decreased its concentration and reduced the baseline conductance. This was accompanied by almost 40% enhancement of sensitivity, and an improved baseline stability under gradient conditions [66]. A purpose-built post suppressor has became commercially-available (Dionex “CRD”), although the demand for such a device decreased with the introduction of the modern hydroxide-selective anion-exchange columns [19].

Table 1.1 Comparison between two suppression methods by Dionex micromembrane suppressors.

	Electrolytic suppression	***Chemical suppression***
Technology released **Latest version released**	1992 (ASRS) 2008 (ASRS-300)	1985 (AMMS) 2008 (AMMS-300)
Suppression control	Applied current	Regenerant concentration and flow-rate
Method Advantages	• "Green" (water in and out) • Automated and simple to operate • No need to prepare reagents • Lower regenerant flow and waste	• Low noise hence low LOD • 100% solvent compatible • Flexible operation due to multiple parameters
Method Disadvantages	• High noise hence higher LOD • Compatible with ≤40% (v/v) solvent • Less flexible (controlled only by applied current) • More susceptible to faults due to dependence on electrical circuit	• Need to prepare regenerant • Requires fine-tuning when changing eluent conditions • High usage of regenerant • Polluting regenerant directed to waste • Longer equilibration time

1.4.2. Ion replacement following ion-exclusion separation

Ion replacement techniques were first applied in ion-exclusion chromatography. Since the eluent in ion-exclusion is a dilute strong acid, weak acid analytes elute only partly ionised and the small degree of dissociation results in insensitive and non-linear conductivity response. However, passing the effluent through a cation-exchange column to replace the hydrogen with a suitable cation can improve the dissociation of the analyte and enhance its conductivity.

Tanaka and Fritz improved the conductivity signal of carbonic acid 10-fold with a series of ion conversions. Consider the bicarbonate analyte which is eluted from a separation column as carbonic acid. This was first converted by a cation-exchange column in the potassium form (equivalent to a suppressor) to potassium carbonate and then, by an anion-exchange column in the hydroxide form, to the more conducting potassium hydroxide [67]. The degree of signal enhancement recorded for different analytes by post-suppression reaction is specified in Table 1.2, and the details of each method are summarised in Table 1.3, both located in Section 1.4.5. Murayama and co-authors [68] gained up to 100-times enhancement for various mono and dicarboxylic acids, using a strong cation-exchange suppressor with pH neutral (sulfates) or alkaline (hydroxides) regenerants. They found that higher enhancements were achieved for acids with higher pK_a values, which accompanied an increasing number of carbon atoms in the analyte. The pH of the solution, governed by the suppressant composition and concentration, was the most important parameter for the peak intensity and shape. When alkaline regenerants between 10 mN and 100 mN were used, the hydroxide ion penetrated through the cation-exchange membrane tube despite the Donnan exclusion effect, with the penetration being greater for the smaller radius counter cations: lithium > sodium > potassium. Introduction of hydroxide at these levels resulted in high pH and background conductivity, accompanied by a reduction in the peak enhancement factor.

Using a similar system configuration, Haginaka and co-authors [69] applied more concentrated alkaline solutions (100-700 mM) as the suppressor regenerant, enhancing the peak area by more than a factor of 2 compared to the suppression performed by Rocklin *et al*. [31]. As in Murayama's work, Haginaka found that Donnan membrane leakage occurred, accompanied by elevation of the baseline. However, it was observed that above a certain concentration of introduced base, the mechanism underlying the enhancement changed, and the response was now a decrease in conductivity producing "negative" peaks (indirect conductivity) rather than positive peaks (direct conductivity) [69]. These phenomena were explained by a quantitative acid-base reaction between the eluted acid and the introduced hydroxide, described by Equation 1.18:

$$OH^- + HX \rightarrow X^- + H_2O \qquad (1.18)$$

The improved sensitivity was, hence, due to the greater limiting equivalent ionic conductance of hydroxide ion compared with carboxylic acid ion, and the yielded negative peaks arose when the hydroxide in the eluent stream was replaced by the analyte anion [19].

1.4.3. Ion replacement following ion-exchange separation

Rocklin, Slingsby and Pohl demonstrated the advantages of the first commercially-available micromembrane suppressors (MMS), by showing a reduction in background conductivity of a dilute acid eluent and increased ionisation and signal intensity of weak carboxylic acids [31,70].

Suppressed IC is the preferred analytical method for the determination of strong anions and moderately weak acids, yet, it presents a problem for weakly dissociated anions if conductivity detection is employed. Similarly to ion-exclusion, the products of suppression for species with a pK_a >5 are neutral or only weakly ionised, and very weak acids of pK_a above 7 are practically undetectable by suppressed conductivity [16,18,19]. Apart from the poor sensitivity, weak acids produce non-linear calibration due to changing dissociation levels [18,71]. Several approaches for post-suppression signal enhancement through modification of the eluted solutes have been studied, utilising various ion-replacement devices [72-81], as summarised in Tables 1.2 and 1.3. Some of the post-suppression reactions are based on previous studies employing non-conductivity detection methods such as absorbance detection, and these are not detailed here.

Dasgupta and co-workers introduced two-dimensional conductivity detection in IC, where the first dimension was a standard suppressed system with subsequent measurement of conductivity [72-75,79,81]. In the second dimension, the suppressed eluent underwent a chemical reaction with an introduced reagent, and the converted eluent was then measured by a second conductivity detector. The concept of the tandem suppressed-non suppressed IC system enabled the simultaneous analysis of highly conducting species on the first detector, along with enhancement of weak acids on the second detector. It was also utilised as a preliminary tool for identification of eluted acids, using the ratio between the two detectors signals as a fingerprint for a pK_a range, rather than relying on retention time alone. During more than a decade of

successive research, various post-column reactors were designed and fabricated in Dasgupta's laboratory, applying different conductivity manipulations, supported by extensive theoretical models and calculations.

The first attempt at conductivity enhancement in this series of experiments was the conversion of suppressed analytes to base (as NaOH) through a sequential ion-exchange process [72], using the same sequential conversion concept as demonstrated for ion-exclusion chromatography by Tanaka and Fritz [67]. The acid analytes after suppression were first converted to a salt (HX → NaX) by cation-exchanger membrane tube, and then to base (NaX → NaOH) by anion-exchanger, both immersed in an external bath containing NaOH solution. Very weak acids suffered from low conversion efficiency, due to the NaX-HX buffer system which inhibited further ionisation of HX once NaX was formed. The method was therefore modified to allow simultaneous conversion of the suppressed acids to alkali-metal halide salts (such as LiF) with the salt reagent flowing through a dual-membrane converter device [73]. Despite being advantageous over standard suppressed conductivity, this process still showed low conversion efficiencies for very weak acids and also caused significant band broadening with insufficient limits of detection. The method of enhancement via conversion of suppressed acids to salts was further modified to allow base-introduction through an electrodialytic NaOH generator device [74]. This principle is the same as described in Equation 1.18, by promoting significant ionisation and conductance of eluted acids with pK_a ≤10, by elevation of the suppressed eluent pH, ideally to at least pH 10 (100 µM hydroxide, producing 20-30 µS baseline). As the authors explained, at the time of the research there was no known method to apply accurate incomplete suppression that would yield precise and constant background of, for example, 100 µM NaOH, which is equivalent to suppressing exactly 99.9% of a 100 mM NaOH eluent. Therefore, the preferred approach was to firstly fully suppress the eluent, and then re-introduce a constant stream of basic reagent into the suppressed eluent. This also enables the application of gradient elution profile for the separation, which can act independently of the applied post-suppression reaction. The reagent, though, should be maintained accurately at a low concentration required for stoichiometric neutralisation of the acid impurities in the suppressed eluent as well as the acid analytes. It was found that base introduction in a small but constant amount was best accomplished by electrodialysis

through a home-made membrane device, named by the authors "MNG"- micro-electrolytic NaOH generator (later termed "MENG"). As a result of the base-introduction and replacement of baseline hydroxide with analyte anion, the converted signal was a negative peak for the analyte on a background of the more conducting base-modified eluent (hence resulting in indirect detection). After introduction of the basic reagent to achieve a pH of 10, the conductivity response of an n-protic acid *A* with $pK_{a\,n} \leq 8$ is given in Equation 1.19 (adapted from [75]):

$$G_{elution} = \frac{(\lambda_{OH} - \lambda_A) \cdot C_A}{10^{-3} \cdot K} \quad (1.19)$$

However, an analyte with pK_a above 8 would not be completely ionised at pH 10, therefore the response will depend on both the concentration and the dissociation constant, and consequently would not be linear. The conversion of an acidic analyte to salt resulted in enhancement of the conductivity of weak acids with a pK_a above 7 by at least one order of magnitude, and enabled the detection of very weak acids (pK_a >9) that could not be detected with conventional suppressed conductivity. For analytes with pK_a value above 10, higher concentrations of introduced base would be required due to the low degree of ionisation of those analytes. When observing a case of stronger acids (pK_a ≤5), their conversion to salts reduced the conductivity response by a factor of 2, since the limiting equivalent ionic conductance is the highest for the acid form (λ_{H^+}=350 S·cm^2·equiv^{-1}; λ_{Na^+}=50 S·cm^2·equiv^{-1}), and as they are fully dissociated after suppression, the maximum conductance was for the acid form in a background of water. Again, with the application of two-dimensional detection, the analysed acids can range from low to high pK_a, with good limits of detection (ppb levels) either before or after the post-suppression reaction.

With the developments in suppressed IC and improved tubular micro-electrolytic base generators, low limits of detection were achieved after basic reagent introduction for acids across a wider pK_a range, as detailed in Table 1.2 [75]. The enhanced response also exhibited good linearity, and for weaker analytes better linearity compared to the suppressed detection response. Peak co-elution could be diagnosed by comparison of the first and second dimensions, particularly if the co-eluting analytes differed in pK_a or limiting equivalent ionic conductance. In addition, compatibility with gradient elution was possible with the use of an impurity anion trap column before the injection valve.

The robust and easily-fabricated planar "MENG" was superior to the former tubular device in terms of induced dispersion, Faradaic efficiency and background noise [79].

Further reduction in noise level and band dispersion was achieved with the latest design – a filament-filled annular helical reactor. Unlike the electrolytic device for base generation and introduction used formerly, the new design facilitated passive introduction of generated basic reagent as the means of controlled penetration through the Donnan exclusion barrier formed in the device [81]. The advantages of this design were attributed to a very effective mixing of the introduced base with the eluent stream, which also contributed to increased repeatability. In electrodialytic mode, the background noise, an important factor for low limits of detection, was found to be linearly proportional to the applied current and less influenced by the type of membrane used in the device. This may suggest that the noise mainly originates in micro-bubbles of electrolytically-produced gas, the amount of which is proportional to the applied current. Therefore, passive introduction of base can produce less noise, especially in the recommended low concentration range (~100 μM). The penetration rate of base through the membrane by overcoming the Donnan effect on its surface correlates to the feed concentration and depends on the nature of the cation. The order of the penetration rate of the examined species was LiOH > NaOH > KOH > ScOH. The highest penetration rate was recorded with the smallest ion, reflecting its low affinity for the ion-exchange site, leading to faster clearance of the membrane on the receiver side. The most dramatic effect on penetration rate was the membrane type. While the counter-ion impact did not exceed a 3-fold change in the rate of transport, the use of a thin Teflon membrane, for example, increased the penetration rate by more than 30-fold, compared to the Nafion membrane.

To conclude Dasgupta's work, the use of post-suppressor reactions for conductivity signal enhancement of weak acids proved to be applicable and beneficial, only when conducted on home-made devices but not with commercially-available suppressors. Since the developed approaches were not followed by commercial devices, they were not established in the scientific community despite the potential market niche.

Another ion-replacement method for conductivity enhancement of weak acids was developed by Caliamanis *et al*. [76-78,80]. Unlike Dasgupta and co-workers, who

aimed at indirect conductivity detection via the introduction of alkaline hydroxide for acid titration, the authors in this approach employed direct conductivity for signal enhancement. Alkaline cations alone, supplied through a cation-exchange membrane, replace the hydrogen ion of partly ionised weak acids, thus converting the weak acids to dissociated salts with higher conductance. This method of enhancement targeted weak acids at high concentrations, where the acid was less ionised and therefore less conducting, so that the conversion becomes most beneficial. For this purpose, the system incorporated two Dionex micromembrane suppressors in series: the first performed conventional chemical suppression of the eluent, while the second operated as an ion-replacement reactor, with sodium hydroxide or disodium EDTA as the regenerant. The analytes were mostly weak inorganic acids, such as fluoride, borate and cyanide, prepared in the eluent and not in water, to eliminate the water negative peak at the void. In preliminary experiments 1 mM NaOH was used as an ion-replacement reagent, leading to very good response for borate compared to conventional suppressed conductivity. In contrast, fluoride and acetate under the same conditions showed a steady decrease in signal as the concentration of NaOH regenerant increased. An increase in the NaOH regenerant concentration also elevated the background conductivity, indicating a leakage of hydroxide across the cation-exchange membrane despite the anion-exclusion effect of the Donnan membrane. The mechanism the authors aimed at included solely the introduction of sodium cations, without an un-controlled introduction of hydroxide, which would elevate the conductivity baseline and react with the acid analytes.

In order to prevent the counter-ion penetration, they chose disodium EDTA as the regenerant, which is a complex molecule that would not easily cross the suppressor membrane. Disodium EDTA at a wide range of concentrations was adjusted with NaOH to various pH levels (5-11), resulting in low background conductivity. The increase in sensitivity for boric acid, using EDTA at pH 7-9, was very close to the enhancement obtained with the NaOH regenerant alone. Further signal improvement of about 20% was possible with EDTA adjusted to pH 11. In contrast, hydrofluoric and acetic acids showed substantial decreases (about 5 fold) when EDTA was used as a regenerant, and carbonic acid showed only a moderate (~50%) increase in peak height [76]. The pH and concentration of the EDTA regenerant and the eluent flow-rate were optimised, to

produce the most efficient conversion of boric acid to sodium borate, which was used as a model for weak acids. One key finding was that higher residence time allowed greater conversion of boric acid to the more conducting borate, but was less efficient in terms of separation time. A drawback of the system was baseline noise due to regenerant pump pulsation. Further optimisation of the disodium EDTA concentration and the pH levels (adjusted by NaOH) demonstrated that above regenerant concentrations of 20 mM disodium EDTA and pH 9, there was a greater diffusion of NaOH through the suppressor membrane. This leakage has been reduced by approximately 15% in new suppressors compared to used ones. The consequence of the elevated levels of NaOH in the eluent was titration of the analyte along with the sulfuric acid suppressant which had leaked across the first suppressor (estimated to be only 5 µM). The NaOH leakage was also accompanied by higher background conductivity and a negative conductivity at the leading and trailing edges of the borate peak. The W-shaped peak led to a conclusion that a more important mechanism for weak acids was the reaction between the analyte and the NaOH leakage, with or without prior ionisation of the weak acid [77].

Subsequent investigations with cyanide, which has the same pK_a as borate, also indicated conductivity enhancement, although it suffered from losses of the volatile analyte through the suppressor membranes [80]. Caliamanis and co-authors [78] also developed a theoretical model to estimate the expected signal enhancement over a particular concentration range. They found that signal enhancement was gained by this PCR method only if the analyte was present above what the authors termed a "critical point concentration (CPC)". The CPC was defined as the concentration in which the acid and the conjugate salt solutions have the same conductivity hence an acid at a concentration below this value will show a higher conductivity after conversion to salt. The logic behind this assertion was that only a weak acid that suffered low dissociation in its acid form will benefit from the dissociation that accompanies an elevation of pH and conversion to its salt. Since the limiting equivalent ionic conductance of any cation is at least 5-times lower than the conductance of hydronium ion, conversion of the acid form to a salt will decrease the overall conductivity of the analyte, unless it was essentially non-dissociated before conversion. The CPC was calculated based on the pK_a of the acids and the limiting equivalent ionic conductance of the ions. The relationship

for monovalent anions with limiting equivalent ionic conductance of 25-75 $S \cdot cm^2 \cdot equiv^{-1}$ is expressed by Equations 1.20 and 1.21:

$$PC \approx (pK_a - 1) \quad (1.20)$$

Where

$$PC = -log\,(CPC) \quad (1.21)$$

As these equations show, the CPC decreases with increasing pK_a, with values of 1.1 mM for sodium benzoate, through to 245 µM for sodium acetate, 6 µM for hydrogen carbonate and 4 nM for sodium borate. For formate, benzoate and acetate, excellent agreement was found between the calculated and experimental CPCs. However, for weaker acids, such as borate, the experimental CPC could not be determined, since the calculated CPC was below the detection limits of the IC system [78]. Nevertheless, the results obtained in two sets of PCR experiments discussed earlier, demonstrated conductivity signal enhancement for concentrations as low as 10 µM for borate, proving it to be above the CPC [76,78].

To conclude the work of Caliamanis and co-workers, their approach could be employed for a range of analytes, mainly inorganic ions, yet the main disadvantage of the method was limited sensitivity and its reliance on suppressors being used for purposes for which they were not specifically designed.

1.4.4. Non-conventional suppression

1.4.4.1. Indirect suppressed conductivity

Zhu and co-authors [82] employed a technique which gave the opposite results of conventional suppressed conductivity detection. In this approach, the eluent was a salt of a strong acid, thus when it underwent suppression, it was converted to a more highly-conducting species. On the elevated background of the suppressed acid eluent, the low-conducting weak acid analytes were detected as negative peaks. This was possible without interference from pH changes or the presence of inorganic ionising substances at a concentration below 400 ppm. The detected analytes ranged from monoprotic and diprotic anions to amino acids, showing good linearity, repeatability and relatively low limits of detection. Despite its potential, this method was not further developed, perhaps due to the requirement to adjust the eluent composition and

strength for both separation needs and detection of each and every analyte, which makes the method less universal.

1.4.4.2. Incomplete suppression

Huang *et al*. introduced a novel approach for enhancement of very weak acids, implementing ion conversion through an acid-base reaction in a single step, thus reducing the dilution effect and band dispersion [83]. As an alternative to full suppression of a hydroxide eluent to water and later introduction of a base reagent through a post-suppressor device, in their approach a single commercially-available micromembrane suppressor was utilised, applying a regenerant at a concentration that was lower than that required for complete suppression. As a consequence, the eluent was just short of completely neutralised, and the residual hydroxide served to ionise the weakly acidic analytes, producing negative peaks on an elevated baseline. The application of this method targeted only very weak acids (pK_a >7) due to the decrease in sensitivity observed after incomplete suppression for carboxylic acids with pK_a values below 7. The target background conductivity was chosen by the principle of keeping it as low as possible, to both reduce noise in the system and maximise the relative analyte signal. Nevertheless, a very low residual hydroxide level may have caused an incomplete titration of the analyte and also disrupted the linearity of response due to varying degrees of dissociation of the analytes. The reported enhancement degree for this approach was approximately 800 times (peak area) compared to suppressed conductivity, yet this was achieved only for a very high analyte concentration of ≥100 ppm. The non-linear conductivity response recorded below this concentration indicated that the reported calculated limit of detection of 100 times lower than that achieved with full suppression, might be far from the actual LOD value.

The authors pointed out some disadvantages of incomplete suppression, including baseline disturbance, long equilibration times (up to 5 h) and inadequate limits of detection. In addition, a major drawback of this method was its incompatibility with gradient elution, due to slow equilibration of the suppressor with varied eluent concentrations. Considering modern separation demands and advanced technology, a detection method that is only suitable for isocratic elution is not very practical, which may be the reason for lack of further development of this method.

1.4.5. Summary of trends in PCR for conductivity signal enhancement

The results of the post-column reactions described in Sections 1.42 through 1.44 are detailed in Table 1.2, and the chromatographic system configurations used in these studies are listed in Table 1.3.

The following general trends are evident from Table 1.2:

- While a decrease in conductivity response was recorded for analytes with pK_a below 7 when PCR was applied after ion-exchange separations, signal enhancement was observed for analytes with higher pK_a [73-77,79-81,83].
- The pK_a cut off for signal enhancement was lower when PCR was applied after ion-exclusion separations, and included carboxylic acids with pK_a of 4.8 [67] or even as low as pK_a 3, although substantial enhancement was still limited to analytes with pK_a >4.2 [68,69].
- The magnitude of signal enhancement was variable under changing PCR conditions and methods.
- The limits of detection reported after PCR were mostly at the 1-10 µM levels, without an obvious trend in the effect of analyte pK_a.

The following general trends are evident from Table 1.3:

- Homemade PCR devices prevailed in ion-exclusion studies [67-69] and also for signal enhancement after suppression in Dasgupta's work [72-75,79,81].
- Commercially-available suppressors were utilised for PCR in Caliamanis' work [76-78,80], and similar suppressed systems without further PCR were utilised in the non-conventional suppression methods [82,83].

Table 1.2 Conductivity response ratio of various acids by post column reaction (PCR).

Analytes	pK_a	*Conc.*	*Vol.*	*Relative Signal (PCR vs. primary signal)*	*LOD*	*Background conductivity*	*comments*	*Ref.*
chloride	<0	1 mM	100 µL	~5% decrease in peak height[a]	n/a	<0.1 µS		[67]
formic acid	3.75	1 mM	100 µL	no change in peak height[a]	n/a	<0.1 µS		[67]
carboxylic acids	~4.8	1 mM	100 µL	~2-fold peak height[a]	n/a	<0.1 µS		[67]
carbonic acid (as $NaHCO_3$)	6.37, 10.32	10 µM - 1 mM	100 µL	10-fold peak height	1.45 µM	<0.1 µS	5-fold peak height after one PCR column; LOD calculated by S/N=2	[67]
malonic acid	2.83,5.69	20 ppm	20 µL	~1.5-fold peak height[a]	n/a	~0.3 µS		[68]
fluoride	3.45	10 ppm	20 µL	~2-fold peak height[a]	n/a	~0.3 µS		[68]
formic acid	3.75	20 ppm	20 µL	4-fold peak height	n/a	~0.3 µS		[68]
carboxylic acids	~4.8	50 ppm	20 µL	40-100 fold peak height	n/a	~0.3 µS	valeric and n-butyric acids were detectable only after PCR	[68]
malonic acid	2.83,5.69	20 ppm	20 µL	30% decreased peak area	2.0 ppm	~30-70 µS[a]	1.4-fold peak area after conventional suppression	[69]
citric acid	3.1,4.8,6.4	20 ppm	20 µL	2.3-fold peak area	1.8 ppm	~30-70 µS[a]	3.1-fold peak area after conventional suppression	[69]
succinic acid	4.21, 5.64	20 ppm	20 µL	27-fold peak area	1.2 ppm	~30-70 µS[a]	21-fold peak area after conventional suppression	[69]

[a] Estimated from a chromatogram.

Analytes	pK_a	*Conc.*	*Vol.*	*Relative Signal (PCR vs. primary signal)*	*LOD*	*Background conductivity*	*comments*	*Ref.*
carboxylic acids	4.6-4.9	20 ppm	20 µL	34-93 fold peak area	1-6 ppm	~30-70 µS[a]	PCR enhancement was 3-times higher than conventional suppression	[69]
inorganic anions	<0 - 2	50 µM - 10 mM	63.7 µL or 25 µL	~2-fold decreased peak area	n/a	n/a	less than stoichiometric conversion for all concentrations	[72]
citrate	3.1,4.8,6.4	50 µM - 10 mM	25 µL	~2-fold peak area[b]	n/a	n/a		[72]
malic acid	3.4,5.1	50 µM - 10 mM	25 µL	~3-fold peak area[b]	n/a	n/a		[72]
formate glycolate	~3.8	50 µM - 10 mM	25 µL	similar peak area	n/a	n/a		[72]
succinate	4.21, 5.64	50 µM - 10 mM	25 µL	~5-fold peak area[b]	n/a	n/a		[72]
acetate propionate	4.75 4.87	50 µM - 10 mM	25 µL	~2-fold peak area	n/a	n/a		[72]
borate	8.9	50 µM -	25 µL	~4-fold peak area	n/a	n/a	very low peak area for borate	[72]

[b] Estimated from a graph.

Analytes	pK_a	*Conc.*	*Vol.*	*Relative Signal (PCR vs. primary signal)*	*LOD*	*Background conductivity*	*comments*	*Ref.*
cyanide	9.31	10 mM						
carboxylic acids inorganic anions	0 - 3	50 µM-10 mM	25µL	4-5-fold decrease in peak area[b]	n/a	~5 µS [b]		[73]
malonic acid	2.83,5.69	50 µM -	25 µL	2-fold decrease in peak area[b]	n/a	~5 µS [b]		[73]
azide	4.72	10 mM						
acetate	4.75	50 µM -	25 µL	~50% decrease in peak area[b]	n/a	~5 µS [b]		[73]
propionate	4.87	10 mM						
succinate	4.21,5.64							
borate	8.91	1.5 mM	25 µL	2-fold peak area[b]	n/a	~8 µS [b]	direct conductivity: enhancement with 65 mM LiF regenerant	[73]
borate	8.91	1.0 mM	25 µL	>350-fold peak area[b]	n/a	~13 µS [b]	indirect conductivity: enhancement with 10 mM LiOH regenerant	[73]
inorganic anions	<0 - 2	25 µM	25 µL	decrease of 3-5-fold in peak height[a,b]	n/a	20-30 µS	baseline noise level <20 nS	[74]
arsenate	2.22, 6.98, 11.50	25 µM	25 µL	decrease of ~2-fold in peak height[a,b]	n/a	20-30 µS	only pK_{a1} and pK_{a2} affect the conversion and conductivity	[74]

Analytes	pK_a	*Conc.*	*Vol.*	*Relative Signal (PCR vs. primary signal)*	*LOD*	*Background conductivity*	*comments*	*Ref.*
carboxylic acids	2.8 - 3.3	25 µM	25 µL	decrease of ~4-fold in peak height[a]	n/a	20-30 µS		[74]
fluoride	3.45	25 µM	25 µL	decrease of ~20% in peak height[a,b]	n/a	20-30 µS		[74]
carbonate	6.37, 10.32	n/a	25 µL	increase of ~2-5-fold in peak height [a,b]	n/a	20-30 µS		[74]
arsenite, silicate, borate	8.9 - 9.8	0-1 mM	25 µL	n/a	2-3 µM	20-30 µS	no signal was detected in suppressed conductivity	[74]
inorganic anions	<0 - 1	10-500 µM	25 µL	decrease of 2-4 fold in peak height[b]	1.5-1.7 µM	~25 µS		[75]
inorganic anions	2 - 3.1	10-500 µM	25 µL	decrease of 4-fold in peak area[b]	2.1-2.7 µM	~25 µS		[75]
halide-acetic acids	0.2 – 2.9	10-500 µM	25 µL	3-4 fold decrease in peak height[a] or area[b]	n/a			[75]
azide	4.72	10-500 µM	25 µL	decrease of 3-fold in peak height[a]	3.0 µM	~25 µS		[75]
phthalate	2.95,5.41	10-500 µM	25 µL	2-fold decrease in peak height[a] and area[b]	1.2 µM	~25 µS		[75]
fumarate	3.03,4.44	10-500 µM	25 µL	~3-fold decrease in peak height[a]	n/a	~25 µS		[75]

Analytes	pK_a	*Conc.*	*Vol.*	*Relative Signal (PCR vs. primary signal)*	*LOD*	*Background conductivity*	*comments*	*Ref.*
citrate	3.1, 4.8,6.4	10-500 µM	25 µL	decrease of about 50% in peak height[a]	n/a	~25 µS		[75]
succinate	4.21, 5.64	10-500 µM	25 µL	decrease of 20-50% in peak height[a] and area[b]	1.7 µM	~25 µS		[75]
sulfide	6.97	10-500 µM	25 µL	n/a	5.1 µM	~25 µS		[75]
borate	8.91	10-500 µM	25 µL	n/a (coeluted)	8.6 µM	~25 µS	no signal was detected in suppressed conductivity	[75]
arsenite, cynaide, silicate	9.2 - 9.8	50 µM	25 µL	n/a	3-4 µM	~25 µS	no signal was detected in suppressed conductivity	[75]
halide-acetic acids, inorganic anions	0 - 3	25 µM	25 µL	2-6 fold decrease in peak height[a] and area[b]	n/a	~25 µS		[79]
carboxylic acids	3 – 4.8	25 µM	25 µL	2-4 fold decrease in peak height[a] and area[b]	n/a	~25 µS		[79]
arsenite, cynaide, silicate	9.2 - 9.8	50 µM	25 µL	n/a. peak height 0.2-0.5 µS[a]	n/a	~25 µS	no signal was detected in suppressed conductivity	[79]
inorganic anions	1.8-2.0	500 µM	25 µL	2 - 5 fold decrease in peak height[a]	n/a	28 µS		[81]
acetate	4.76	250 µM	25 µL	2-fold decrease in peak height[a]	n/a	28 µS		[81]

Analytes	pK_a	*Conc.*	*Vol.*	*Relative Signal (PCR vs. primary signal)*	*LOD*	*Background conductivity*	*comments*	*Ref.*
sulfide, carbonate	6.97, 6.37, 10.32	250 µM	25 µL	2 to 3-fold increase in peak height[a]	n/a	28 µS		[81]
borate	8.91	0.6 µM - 250 µM	25 µL	n/a. peak height ~2 µS for 250 µM[a]	0.6 µM	28 µS	no signal was detected in suppressed conductivity	[81]
arsenite, cyanide, silicate	9.2 - 9.8	0.6 µM - 250 µM	25 µL	n/a. peak height 1.5-2.2 µS[a]	n/a	28 µS	no signal was detected in suppressed conductivity	[81]
fluoride	3.45	10 µM - 10 mM	50 µL	~ 5-fold decrease	n/a	~2-7 µS	10 mM EDTA regenerant (pH 11)	[76]
acetate	4.76							
carbonic acid	6.37, 10.32	1 mM - 10 mM	50 µL	52% increase in peak height	n/a	~2-7 µS	maximum enhancement achieved at 10 mM analyte	[76]
boric acid	8.91	10 µM - 10 mM	50 µL	765-fold peak height; 1000-fold peak area	10 µM[c]	~5-65 µS	values for 1 mM borate; 1 mM NaOH regenerant	[76]
boric acid	8.91	10 µM - 10 mM	50 µL	877-fold peak height; 231-fold peak area	10 µM[c]	~2-7 µS	values for 1 mM borate; 10 mM EDTA regenerant (pH 11)	[76]
boric acid	8.91	10 µM - 1 mM	20 µL	850-fold peak height; 3400-fold peak area	10 µM[c]	~20 µS	maximal enhancement with 20 mM EDTA regenerant (pH 9)	[77]
cyanide	9.22	10 µM -	20 µL	at least 250-fold peak height	50 µM[c]	n/a	2-10% cyanide loss through the	[80]

[c] Not reported to be calculated by S/N ratio

Analytes	pK_a	*Conc.*	*Vol.*	*Relative Signal (PCR vs. primary signal)*	*LOD*	*Background conductivity*	*comments*	*Ref.*
		1 mM					suppressor membrane	
taurine	1.5,8.74	0-200 ppm	50 µL	n/a	0.5 ppm	n/a	0.75 mM KCl and NaOH (pH 11)	[82]
leucine	2.36,9.60				0.4 ppm[c]		eluent	
tartaric acid	3.05,4.45	0-200 ppm	50 µL	n/a	3.0 ppm	n/a	0.75 mM Na_2SO_4 and NaOH	[82]
malic acid	3.40,5.2				1.3 ppm[c]		(pH 11) eluent	
formic acid	3.75	0-80 ppm	50 µL	n/a	0.2 ppm[c]	n/a	0.75 mM Na_2SO_4 and NaOH (pH 11) eluent	[82]
lactic acid	3.86	0-200 ppm	50 µL	n/a	0.4 ppm[c]	n/a	2 mM KNO_3 eluent	[82]
benzoic acid	4.20							
phenylpropionate	4.37	0-100 ppm	50 µL	n/a	8.3 ppm	n/a	2 mM KNO_3 eluent	[82]
phenol	9.99				0.8 ppm[c]			
malic, glutamic, citric, carbonic acids	<7	n/a	10 µL	decrease in peak height	n/a	n/a	no data presented, only summary	[83]
boric acid	8.91	1.6 mM - 24 mM	10 µL	261-fold peak height; 1002-fold peak area	16 µM	35-40 µS		[83]
arsenous acid	9.29	40 µM - 1.6 mM	10 µL	146-fold peak height; 402-fold peak area	11.9 µM	35-40 µS	arsenous acid hardly retained	[83]

Table 1.3 System details for methods described in Table 1.2.

Ref.	*Column*	*Eluent*	*Suppressor*	*Suppressant*	*Enhancement device*	*PCR regenerant*
[67]	TSK SCX, 5 µm laboratory- packed cation-exchange resin in H^+ form	water at 1 mL/min	laboratory-packed cation-exchange column in K^+ form	-	anion-exchange column in OH^- form.	-
[68]	laboratory- packed strong cation-exchange resin	2 mN H_2SO_4 at 0.4 mL/min or 1.5 mL/min	cation-exchange hollow fibre membrane in a PTFE tubing	1-100 mN of K,Na or LiOH or SO_4 at 2 mL/min	-	-
[69]	Dionex HPICE-AS1 high capacity (for ion-exclusion).	1 mM H_2SO_4 at 0.8 mL/min	Dionex AFS-2 cation-exchange hollow-fibre membrane	10 mM NaOH for normal suppression; 600 mM NaOH for signal enhancement; at 1.5 mL/min	-	-
[72]	Dionex AS 5A	NaOH at 1 mL/min	filament-filled helical tubular nafion membrane suppressor externally resin-packed	~20 mM dodecylbenzene-sulfonic acid at 1 mL/min	membrane-based or packed column dual converter	10 mM NaOH at ~1 mL/min.
[73]	Dionex AS 5A	NaOH at 1 mL/min	filament-filled helical tubular nafion membrane	~20 mM dodecylbenzene-sulfonic acid at 1 mL/min	home-made dual-membrane ion-	10 mM LiF with 1 mM $NH_4F{\cdot}HF$

Ref.	*Column*	*Eluent*	*Suppressor*	*Suppressant*	*Enhancement device*	*PCR regenerant*
			suppressor externally resin-packed		exchange converter	at 1-2 mL/min
[74]	Dionex AS 5A	19 mM NaOH at 1 mL/min	filament-filled helical tubular nafion membrane suppressor externally resin-packed	~20 mM dodecylbenzene-sulfonic acid at 1 mL/min	home-made "MNG" (microelectrodialytic NaOH generator)	10 mM NaOH
[75]	Dionex IonPac AS11 4 mm	3-30 mM NaOH	Dionex ASRS-I	water	tubular Home-made "MENG"	10 mM NaOH
[79]	Dionex IonPac AS11 4 mm	3-30 mM NaOH	Dionex ASRS-I	water	planar Home-made "MENG"	10 mM NaOH
[81]	Dionex IonPac AS11-HC 4 mm	0-30 mM KOH gradient	electrolytic suppressor (unspecified)	water	various membrane home-made devices, used in passive or in electrodialytic mode	50-100 mM KOH at 0.5 mL/min
[76]	Dionex IonPac AS4A-SC 4 mm	5 mM NaOH at 1 mL/min	Dionex AMMS- II	12.5 mM H_2SO_4	Dionex AMMS II	1-30 mM NaOH or 100 mM Na_2EDTA
[77]	Dionex IonPac AS11 4 mm	5 mM NaOH at 0.2-1 mL/min	Dionex AMMS- II	50 mM H_2SO_4 at 1.2 mL/min	Dionex AMMS II	1-100 mM Na_2EDTA (pH 5-11), at

Ref.	*Column*	*Eluent*	*Suppressor*	*Suppressant*	*Enhancement device*	*PCR regenerant*
						1.2 mL/min
[80]	Dionex IonPac AS11 4 mm	5 mM NaOH at 0.2 or 1 mL/min	Dionex AMMS- II	50 mM H_2SO_4 at 1.2 mL/min	Dionex AMMS II	20 mM Na_2EDTA (pH 9), at 1.2 mL/min
[82]	Dionex IonPac AS4A-SC	0.75 mM KCl or Na_2SO_4 (pH 11.5 with NaOH) or 2 mM KNO_3 at 2 mL/min	Dionex ASRS	n/a	-	-
[83]	Dionex IonPac AS11 4 mm	1 or 4 mM NaOH at 1 mL/min	Dionex ASRS-I	0.1 mM or 0.4 mM H_2SO_4 at 1 mL/min	-	-

1.5. Analysis of pharmaceuticals by ion-exchange chromatography

The analytes requiring measurement in the pharmaceutical field include raw materials, intermediates formed during different stages of R&D and production, drug substances, active and non-active ingredients. In order to comply with the heavy degree of regulation in the pharmaceutical area, there is an emphasis on the determination of degradation products, impurities and contaminants in the pharmaceutical preparation, such as traces of cleaning solutions used in the production equipment. In addition, environmental concerns require the determination of traces in waste streams of the pharmaceutical production process [6].

Ion-exchange chromatography has been employed in the pharmaceutical industry, mainly during the early stages of drug development [4]. Naturally suitable for charged compounds, ion-exchange is useful for the trace determination of impurities, as well as determination of counter-ions of the active component [1,7]. Less common is the application of IC for analysis of active pharmaceutical ingredients, as demonstrated in Table 1.4.

1.6. Aims of this project

This review has emphasised the requirement for alternative detection methods of weak organic ions after separation by IC, to address analysis requirements in the pharmaceutical industry.

As demonstrated in the literature, post-column reactions provided conductivity signal enhancement of weak acids after suppression, but without significant success at low analyte concentration when utilising commercially-available suppressors as PCR devices. The first aim of this project was to understand the potential of the PCR approach on a set of weak acid analytes. Once the approach showed potential for signal enhancement, the usage of a suppressor as a PCR device had to be further explored, and alternatives for introduction of reagent developed, if a suppressor proved inefficient for this purpose. The chosen PCR methods also had to comply with chromatographic conditions required in this work, which was the separation of weakly-charged hydrophobic analytes by eluents containing moderate concentrations of organic solvents.

The latter operational constraints led to the second aim of this work, which was an investigation into the compatibility of the components of a commercial IC instrument (particularly the suppressor) to conditions of aqueous/solvent gradient and for determination of hydrophobic target analytes of pharmaceutical relevance. No comprehensive studies have been conducted into the utility of IC for these purposes, and the few published works have concentrated on aspects of application rather than performance of the system.

The final goal of this work was to implement the gathered operational recommendations from the previous stages, for successful determination of pharmaceutically-related compounds by coupling IC with universal detection systems. Since the pharmaceutical industry requires the use of several separation techniques to ensure maximal probability of impurity detection, it was necessary to provide a proof of concept for interfacing IC with advanced universal detectors, such as mass spectrometry and nebulising detectors.

Table 1.4 Application of ion-exchange chromatography for the determination of active ingredients and impurities in pharmaceutical preparations. Detection was performed using conductivity (CD); pulsed amperometric detection (PAD), mainly with gold working electrode; UV absorbance (UV); and refractive index (RI). Detection was conducted with or without post-column reaction (PCR).

Pharmaceutical classification	*Analyte*	*Column*	*Eluent*	*Detection*	*Ref.*
Bone disease treatment					
bisphosphonates	alendronate	Waters IC-Pak A HR or Dionex Omni-Pac PAX-100	~1.5 mM HNO_3 in 20% ACN	Direct CD	[84]
	alendronate, clodronate, etidronate	Waters IC-Pak A HR	1-12 mM HNO_3 in 20% ACN	Indirect UV	[85]
	clodronate	Dionex IonPac AS7	40 mM HNO_3	UV after PCR	[86]
	pamidronate	Alltech universal anion	5 mM KNO_3	RI	[87]
	alendronate, clodronate, etidronate	Hamilton PRP-X100	1 mM trimesic acid (pH 5.5)	Indirect UV	[88]
	pamidronate, etidronate	Waters IC-Pak A	2 mM HNO_3 or 25 mM succinic acid	Direct CD	[89]
	alendronate, clodronate,	Phenomenex Phenosphere SAX	20 mM sodium citrate (pH 3.6)	Indirect UV	[90]
	pamidronate, etidronate	Phenomenex Sphereclone SAX	20 mM sodium citrate (pH 4.6)	Indirect UV	[90]
Cardiovascular agents					
beta adrenergic blockers	alprenolol, acebutolol, atenolol, propranolol, oxprenolol	Waters IC-Pak C M/D	50 mM HNO_3 in 4% ACN	UV	[91]

Pharmaceutical classification	*Analyte*	*Column*	*Eluent*	*Detection*	*Ref.*
	propranolol	Dionex IonPac CS-14	20–75 mM MSA in 40–75% MeOH	UV	[92]
phosphodiesterase inhibitor	dipyridamole				
Sympathomimetic drugs (including Alpha/Beta adrenergic agonists)	salbutamol, fenoterol, clenbuterol, clorprenaline	Metrohm Metrosep C 1-2	1.8 mM HNO3 in 2% ACN	Direct CD	[93]
	ephedrine, pseudoephedrine, norephedrine	Metrohm Metrosep C 1-2	2 mM HNO3 in 2% ACN	Direct CD	[94]
	norepinephrine , epinephrine, dopamine	Metrohm Metrosep C 1-2	1 mM HNO_3	Direct CD	[95]
Diuretics and anti-hypertensive agents					
	chlorothiazide, furosemide, althiazide, trichloromethiazide, captopril	Dionex IonPac AS-20	50-100 mM KOH in 25% MeOH	UV	[96]
	chlorothiazide, furosemide	Dionex IonPac AS-11	30-70 mM KOH in 25-75% MeOH	UV	[92]
Analgesics (non-narcotic)					
	paracetamol, salicylic acid	Waters IC-Pak A HR	5 mM LiOH in 5% ACN	UV	[97]
non-steroidal anti-	ibuprofen, naproxen, fenbufen,	Dionex IonPac AS-20	20-100 mM KOH in 25% MeOH	UV	[96]

Pharmaceutical classification	*Analyte*	*Column*	*Eluent*	*Detection*	*Ref.*
inflammatory drugs (NSAID)	sulindac, acetylcalicylic acid, ketoprofen, indomethacine				
	ibuprofen, mefenamic acid, flufenamic acid, tolfenamic acid, diclofenac	Dionex IonPac AS-11	30-70 mM KOH in 25-75% MeOH	UV	[92]
Anti-Bacterial agents					
aminoglycosides Antibiotics	neomycin	Dionex CarboPac PA1	2.4 mM NaOH	PAD	[98]
	tobramycin	Dionex CarboPac PA1	2 mM KOH	PAD	[99]
	streptomycin, dihydrostreptomycin	Dionex CarboPac PA1	70 mM NaOH	PAD	[100]
	gentamicin	Dionex CarboPac PA1	3-5 mM NaOH	PAD after PCR	[101]
	paromomycin	Dionex CarboPac PA1	1.8 mM KOH	PAD	[102]
tetracycline Antibiotics	oxytetracycline, tetracycline, chlortetracycline, doxycycline	Dionex OmniPac PCX-100	200 mM HCl in 28% ACN	UV	[103]
beta -lactam antibiotics	cephalosporin (cefepime) (degradation products)	Dionex IonPac CS-17	6-85 mM MSA	Suppressed CD	[104]
	flucloxacillin, amoxicillin	Agilent ZORBAX 300-SCX	25 mM $NH_4H_2PO_4$ (pH 2.6) in 5% ACN	UV	[105]

Pharmaceutical classification	*Analyte*	*Column*	*Eluent*	*Detection*	*Ref.*
Anti-viral treatment					
	indinavir (ionic impurities)	Metrohm Metrosep A Supp5	3.2 mM Na_2CO_3 with 1 mM $NaHCO_3$	Suppressed CD	[106]
	foscarnet	Waters IC-Pak A	2 mM HNO_3 or 25 mM succinic acid	Direct CD	[89]
Anti-infective agents mucolytic drugs					
	carbocysteine	Dionex IonPac CS-14	0.25 mM trifluoroacetic acid	Suppressed CD	[107]
Antihistamines					
	diphenhydramine, doxepine	Dionex IonPac CS-14	20–75 mM MSA in 40–75% MeOH	UV	[92]
	brompheniramine, cyclizine, chlorcyclizine, pheniramine, chlorpheniramine, meclizine. pyrrobutamine, thenyldiamine, thonzylamine,	ZirChrom PBD-ZrO_2 (Lab-packed)	25 mM potassium phosphate buffer (pH 7.0) in 40% ACN	UV	[108]

1.7. References

[1] P.R. Haddad, P.E. Jackson, Ion chromatography: principles and applications, Elsevier, Amsterdam, 1990.

[2] W.T. Frankenberger Jr, H.C. Mehra, D.T. Gjerde, J. Chromatogr. A 504 (1990) 211.

[3] B. Lopez-Ruiz, J. Chromatogr. A 881 (2000) 607.

[4] J. Weiss, Ion Chromatography, Wiley-VCH, Weinheim, 2nd ed., 1995.

[5] United States Environmental Protection Agency (EPA), *Index to EPA Test Methods*, 2003, retrieved 10 December 2011, <http://www.epa.gov/region1/info/testmethods/pdfs/testmeth.pdf>.

[6] D. Jenke, J. Chromatogr. Sci. 49 (2011) 524.

[7] J.S. Fritz, D.T. Gjerde, Ion Chromatography, Wiley-VCH, Weinheim, 4th ed., 2009.

[8] Y.C Lee, J. Chromatogr. A 720 (1996) 137.

[9] T.R.I. Cataldi, C. Campa, G.E. De Benedetto, Fresenius. J. Anal. Chem. 368 (2000) 739.

[10] P. Haddad, Anal. Bioanal. Chem. 379 (2004) 341.

[11] P.R. Haddad, P.N. Nesterenko, W. Buchberger, J. Chromatogr. A 1184 (2008) 456.

[12] R.D. Rocklin, C.A. Pohl, J. Liq. Chromatogr. 6 (1983) 1577.

[13] A.P. Clarke, P. Jandik, R.D. Rocklin, Y. Liu, N. Avdalovic, Anal. Chem. 71 (1999) 2774.

[14] Y. Ding, H. Yu, S. Mou, J. Chromatogr. A 982 (2002) 237.

[15] H. Yu, Y. Ding, S. Mou, P. Jandik, J. Cheng, J. Chromatogr. A 966 (2002) 89.

[16] W.W. Buchberger, P.R. Haddad, J. Chromatogr. A 789 (1997) 67.

[17] P. Jandik, P.R. Haddad, P.E. Sturrock, Crit. Rev. Anal. Chem. 20 (1988) 1.

[18] P.K. Dasgupta, J. Chromatogr. Sci. 27 (1989) 422.

[19] P.R. Haddad, P.E. Jackson, M.J. Shaw, J. Chromatogr. A 1000 (2003) 725.

[20] R.M. Wheaton, W.C. Bauman, Ind. Eng. Chem. Res. 45 (1953) 228.

[21] K. Tanaka, T. Ishizuka, H. Sunahara, J. Chromatogr. A 174 (1979) 153.

[22] J. Stillian, LC 3 (1985) 802.

[23] D.T. Gjerde, J.S. Fritz, G. Schmuckler, J. Chromatogr. A 186 (1979) 509.

[24] D.T. Gjerde, G. Schmuckler, J.S. Fritz, J. Chromatogr. A 187 (1980) 35.

[25] H. Small, T.S. Stevens, W.C. Bauman, Anal. Chem. 47 (1975) 1801.

[26] C.A. Lucy, J. Chromatogr. A 1000 (2003) 711.

[27] T.S. Stevens, J. Chromatogr. A 956 (2002) 43.

[28] T.S. Stevens, J.C. Davis, H. Small, Anal. Chem. 53 (1981) 1488.

[29] Y. Hanaoka, T. Murayama, S. Muramoto, T. Matsuura, A. Nanba, J. Chromatogr. A 239 (1982) 537.

[30] T.S. Stevens, G.L. Jewett, R.A. Bredeweg, Anal. Chem. 54 (1982) 1206.

[31] R.D. Rocklin, R.W. Slingsby, C.A. Pohl, J. Liq. Chrom. Relat. Tech. 9 (1986) 757.

[32] W.R. Jones, P. Jandik, A.L. Heckenberg, Anal. Chem. 60 (1988) 1977.

[33] P.E. Jackson, C.A. Pohl, Trends Anal. Chem. 16 (1997) 393.

[34] J.R. Stillian, V. Barreto, K. Friedman, S. Rabin, M. Toofan, US Patent 5248426 (1993).

[35] Z.W. Tian, R.Z. Hu, H.S. Lin, J.T. Wu, J. Chromatogr. 439 (1988) 159.

[36] D.L. Strong, P.K. Dasgupta, Anal. Chem. 61 (1989) 939.

[37] D.L. Strong, C.U. Joung, P.K. Dasgupta, J. Chromatogr. A 546 (1991) 159.

[38] S. Rabin, J. Stillian, V. Barreto, K. Friedman, M. Toofan, J. Chromatogr. A 640 (1993) 97.

[39] S. Rabin, J. Stillian, J. Chromatogr. A 671 (1994) 63.

[40] SRS 300 product manual (Document 031956-06), Dionex Corp., Sunnyvale, CA, USA, 2008.

[41] Y. Liu, K. Srinivasan, C. Pohl, N. Avdalovic, J. Biochem. Biophys. Meth. 60 (2004) 205.

[42] D.L. Strong, P.K. Dasgupta, K. Friedman, J.R. Stillian, Anal. Chem. 63 (1991) 480.

[43] D.L. Strong, P.K. Dasgupta, J. Membr. Sci. 57 (1991) 321.

[44] H. Small, Y. Liu, N. Avdalovic, Anal. Chem. 70 (1998) 3629.

[45] Y. Liu, N. Avdalovic, C.A. Pohl, R. Matt, H. Bhillon, R.E. Kiser, Am. Lab. 28 (1998) 48.

[46] ICS-2000 Ion Chromatography Data Sheet (Document LPN 1500-07), Dionex Corp., Sunnyvale, CA, USA, 2008.

[47] K. Vermeiren, J. Chromatogr. A 1085 (2005) 66.

[48] P.E. Jackson, D.H. Thomas, B. Donovan, C.A. Pohl, R.E. Kiser, J. Chromatogr. A 920 (2001) 51.

[49] Z. Lu, Y. Liu, V. Barreto, C. Pohl, N. Avdalovic, R. Joyce, B. Newton, J. Chromatogr. A 956 (2002) 129.

[50] S. Pelletier, C.A. Lucy, J. Chromatogr. A 1125 (2006) 189.

[51] R. Saari-Nordhaus, J.M. anderson Jr, Am. Lab. 26 (1994) 28.

[52] S. Sato, Y. Ogura, A. Miyanaga, T. Sugimoto, K. Tanaka, H. Moriyama, J. Chromatogr. A 956 (2002) 53.

[53] R. Saari-Nordhaus, J.M. Anderson Jr, J. Chromatogr. A 782 (1997) 75.

[54] R. Saari-Nordhaus, J.M. Anderson Jr, J. Chromatogr. A 956 (2002) 15.

[55] H. Schafer, M. Laubli, P. Zahner, US Patent 6153101 (2000).

[56] J.M. Anderson Jr, R. Saari-Nordhaus, US Patent 6200477 (2001).

[57] W. Huang, R. Hu, H. Chen, Y. Su, Analyst 136 (2011) 901.

[58] D.T. Gjerde, J.V. Benson, Anal. Chem. 62 (1990) 612.

[59] P. Jandik, J. Li, W. Jones, D. Gjerde, Chromatographia 30 (1990) 509.

[60] P.E. Jackson, P. Jandik, J. Li, J. Krol, G. Bondoux, D. T. Gjerde, J. Chromatogr. A 546 (1991) 189.

[61] C.A. Pohl, R.W. Slingsby, J.R. Stillian, R. Gajek, US Patent 4999098 (1991).

[62] MMS 300 product manual (Document 031727-04), Dionex Corp., Sunnyvale, CA, USA, 2008.

[63] C. Pohl, K. Srinivasan, Y. Liu, Personal communication, Dionex Corp., Sunnyvale, CA, USA, 2010.

[64] I.K. Dimitrakopoulos, N.S. Thomaidis, N.C. Megoulas, M.A. Koupparis, J. Chromatogr. A 1217 (2010) 3619–3627.

[65] P. Rantakokko, S. Mustonen, T. Vartiainen, J. Chromatogr. A 1020 (2003) 265.

[66] T. Sunden, A. Cedergren, Anal. Chem. 56 (1984) 1085.

[67] K. Tanaka, J.S. Fritz, Anal. Chem. 59 (1987) 708.

[68] T. Murayama, T. Kubota, Y. Hanaoka, S. Rokushika, K. Kihara, H. Hatano, J. Chromatogr. 435 (1988) 417.

[69] J. Haginaka, J. Wakai, H. Yasuda, T. Nomura, J. Chromatogr. 447 (1988) 373.

[70] R.W. Slingsby, J. Chromatogr. 371 (1986) 373.

[71] P.W. Atkins, Physical Chemistry, Oxford University Press, Oxford, 4th ed., 1990.

[72] I. Berglund, P.K. Dasgupta, Anal. Chem. 63 (1991) 2175.

[73] I. Berglund, P.K. Dasgupta, Anal. Chem. 64 (1992) 3007.

[74] I. Berglund, P.K. Dasgupta, J.L. Lopez, O. Nara, Anal. Chem. 65 (1993) 1192.

[75] A. Sjoegren, P.K. Dasgupta, Anal. Chem. 67 (1995) 2110.

[76] A. Caliamanis, M.J. McCormick, P.D. Carpenter, Anal. Chem. 69 (1997) 3272.

[77] A. Caliamanis, M.J. McCormick, P.D. Carpenter, J. Chromatogr. A 850 (1999) 85.

[78] A. Caliamanis, M.J. McCormick, P.D. Carpenter, Anal. Chem. 71 (1999) 741.

[79] A. Sjögren, P.K. Dasgupta, Anal. Chim. Acta 384 (1999) 135.

[80] A. Caliamanis, M.J. McCormick, P.D. Carpenter, J. Chromatogr. A 884 (2000) 75.

[81] R. Al-Horr, P.K. Dasgupta, R.L. Adams, Anal. Chem. 73 (2001) 4694.

[82] Y. Zhu, S. Wang, W.P Liu, LC GC N. Am. 18 (2000) 200.

[83] Y. Huang, S. Mou, K.-n. Liu, J. Chromatogr. A 832 (1999) 141.

[84] E.W. Tsai, D.P. Ip, M.A. Brooks, J. Chromatogr. A 596 (1992) 217.

[85] E.W. Tsai, S.D. Chamberlin, R.J. Forsyth, C. Bell, D.P. Ip, M.A. Brooks, J. Pharm. Biomed. Anal. 12 (1994) 983.

[86] J.P. Kosonen, J. Pharm. Biomed. Anal. 10 (1992) 881.

[87] J. Quitasol, L. Krastins, J. Chromatogr. A 671 (1994) 273.

[88] R. Thompson, N. Grinberg, H. Perpall, G. Bicker, P. Tway, J. Liq. Chromatogr. 17 (1994) 2511.

[89] J. Den Hartigh, R. Langebroek, P. Vermeij, J. Pharm. Biomed. Anal. 11 (1993) 977.

[90] C. Fernandes, R.S. Leite, Lan, F.M. as, J. Chromatogr. Sci. 45 (2007) 236.

[91] R. Ghanem, M.A. Bello, M. Callejun, A. Guiratim, J. Pharm. Biomed. Anal. 15 (1996) 383.

[92] P. Zakaria, G. Dicinoski, M. Hanna-Brown, P.R. Haddad, J. Chromatogr. A 1217 (2010) 6069.

[93] S. Shen, J. Ouyang, W.R.G. Baeyens, J.R. Delanghe, Y. Yang, J. Pharm. Biomed. Anal. 38 (2005) 166.

[94] J. Ouyang, X. Gao, W.R.G. Baeyens, J.R. Delanghe, Biomed. Chromatogr. 19 (2005) 266.

[95] C.L. Guan, J. Ouyang, Q.L. Li, B.H. Liu, W.R.G. Baeyens, Talanta 50 (2000) 1197.

[96] P. Zakaria, G.W. Dicinoski, B.K. Ng, R.A. Shellie, M. Hanna-Brown, P.R. Haddad, J. Chromatogr. A 1216 (2009) 6600.

[97] J.L. Pérez, M. Angel Bello, Talanta 48 (1999) 1199.

[98] V.P. Hanko, J.S. Rohrer, J. Pharm. Biomed. Anal. 51 (2010) 96.

[99] V.P. Hanko, J.S. Rohrer, H.H. Liu, C. Zheng, S. Zhang, X. Liu, X. Tang, J. Pharm. Biomed. Anal. 47 (2008) 828.

[100] V.P. Hanko, J.S. Rohrer, LC-GC N. Am. 35 (2007) 64.

[101] L.A. Kaine, K.A. Wolnik, J. Chromatogr. A 674 (1994) 255.

[102] Dionex Application note 186, Dionex Corp., Sunnyvale, CA, USA, 2007.

[103] X. Ding, S. Mou, J. Chromatogr. A 897 (2000) 205.

[104] Dionex Application note 205, Dionex Corp., Sunnyvale, CA, USA, 2008.

[105] H. Liu, H. Wang, V.B. Sunderland, J. Pharm. Biomed. Anal. 37 (2005) 395.

[106] S.J. Prasanna, H.K. Sharma, K. Mukkanti, M. Sivakumaran, K.S.R.P. Kumar, V.J. Kumar, J. Pharm. Biomed. Anal. 50 (2009) 1065.

[107] N.C. Megoulas, M.A. Koupparis, J. Chromatogr. A 1026 (2004) 167.

[108] Y. Mao, P.W. Carr, Anal. Chem. 73 (2001) 4478.

Chapter 2

General experimental

This section describes the chemicals and common instrumentation used throughout the work. Specific instrumentation and procedures are described in the relevant chapters, in addition to relevant data on the participating analytes.

2.1. Reagents

The chemicals used in this work are listed in Table 2.1 and were of analytical reagent grade unless specified.

Table 2.1 Chemicals utilised in this work (alphabetic order)

Compound	***Formula***	***Supplier***
Acetic acid, glacial	CH_3COOH	Biolab
Acetonitrile	CH_3CN	Ajax Finechem
Althiazide	$C_{11}H_{14}ClN_3O_4S_3$	Sigma–Aldrich
Ammonium chloride	NH_4Cl	BDH Chemicals
Benzenesulfonic acid	$C_6H_5SO_2OH$	TCI
Benzoate (Na^+ salt)	$C_6H_5COO^-Na^+$	BDH Chemicals
Benzoic acid	C_6H_5COOH	BDH Chemicals
Boric acid	H_3BO_3	BDH Chemicals
Calcium chloride dihydrate	$CaCl_2 \cdot 2H_2O$	Ajax Finechem
Chlorothiazide	$C_7H_6ClN_3O_4S_2$	Sigma–Aldrich
Cinnamic-acid (trans)	$C_9H_8O_2$	BDH Chemicals
Diclofenac (Na^+ salt)	$C_{14}H_{10}Cl_2NO_2^-Na^+$	Sigma–Aldrich
Fenbufen	$C_{16}H_{14}O_3$	Sigma–Aldrich
Flufenamic acid	$C_{14}H_{10}F_3NO_2$	Sigma–Aldrich
Formic acid	HCOOH	Ajax Finechem
Furosemide	$C_{12}H_{11}ClN_2O_5S$	Sigma–Aldrich
Hexanesulfonic acid, 0.1M	$CH_3(CH_2)_5SO_2OH$	Dionex Corp.
4-Heptylbenzoic acid	$C_{14}H_{20}O_2$	Sigma–Aldrich

Compound	*Formula*	*Supplier*
Hydrochloric acid	HCl	Ajax Finechem
Ibuprofen	$C_{13}H_{18}O_2$	Sigma–Aldrich
Indoprofen	$C_{17}H_{15}NO_3$	Sigma–Aldrich
Lithium chloride	LiCl	Ajax Finechem
Magnesium dichloride	$MgCl_2$	Sigma–Aldrich
Mefenamic acid	$C_{15}H_{15}NO_2$	Sigma–Aldrich
Methanol	CH_3OH	Merck
1-Naphthoic acid	$C_{11}H_8O_2$	Sigma–Aldrich
Naproxen	$C_{14}H_{14}O_3$	Sigma–Aldrich
4-Octylbenzenesulfonate (Na^+ salt)	$C_{14}H_{21}O_3S^-Na^+$	Sigma–Aldrich
Phenylacetic acid	$C_8H_8O_2$	Hopkin&Williams
2-Phenylbutyric acid	$C_{10}H_{12}O_2$	Sigma–Aldrich
2-Phenylsuccinic acid	$C_{10}H_{10}O_4$	Sigma–Aldrich
Phosphoric acid	H_3PO_4	Ajax Finechem
Potassium chloride	KCl	BDH Chemicals
Potassium hydroxide	KOH	Sigma–Aldrich
Sodium chloride	NaCl	Merck
Sodium hydroxide	NaOH	Sigma–Aldrich
Succinate (Na^+ salt)	$C_4H_4O_4^{-2}Na^+_2$	BDH Chemicals
Sulfuric acid	H_2SO_4	Ajax Finechem
Sulindac	$C_{20}H_{17}FO_3S$	Sigma–Aldrich
Tolfenamic acid	$C_{14}H_{12}ClNO_2$	Sigma–Aldrich

2.2. Instrumentation

The ion chromatography system employed was a Dionex (Thermo-Fisher Scientific, Sunnyvale, CA, USA) ICS-3000™, consisting of a dual gradient pump unit (DP), dual eluent generator unit EluGen® (EG), autosampler (AS) and dual column and detector compartment (DC). The EluGen was equipped with potassium hydroxide and methanesulfonic acid (MSA) cartridges for electrolytic preparation of eluent, and followed by a continuously-regenerated trap column (CR-TC) and degasser. Organic solvents used in the eluents were introduced after the CR-TC [1] through a 3-port

tee-piece connector (Upchurch Scientific; Oak Harbor, WA, USA), using an additional HPLC pump (Jasco PU-2089i; Easton, MD, USA, or Dionex Ultimate 3000 gradient pump), followed by a gradient mixer (Dionex GM-3, 4 mm). Dionex conductivity detectors were corrected to 35°C with temperature coefficient of 1.7%. All instrument control and data acquisition was achieved through Chromeleon® chromatography management software (version 6.80 or 6.90).

Physico-chemical properties of the test analytes were obtained using ACDLabs™ software version 12.0 (Advanced Chemistry Development Inc., Toronto, Canada). Statistical analysis of the results was performed on Excel™ (Microsoft Corporation, Redmond, Washington, USA), using the analysis ToolPak add-in. An Excel™ in-house derived spreadsheet based on the method of Shellie *et al.* [1,2] was used for retention time modelling. The system configuration was varied between the different experiments, and their details, along with additional pumps and detectors etc. are described in each chapter. Additionally, separation and suppression conditions are detailed in the relevant chapters.

2.3. References

[1] P. Zakaria, G.W. Dicinoski, B.K. Ng, R.A. Shellie, M. Hanna-Brown, P.R. Haddad, J Chromatogr. A 1216 (2009) 6600.

[2] R.A. Shellie, B.K. Ng, G.W. Dicinoski, S.D.H. Poynter, J.W. O'Reilly, C.A. Pohl, P.R. Haddad, Anal. Chem. 80 (2008) 2474.

Chapter 3

Approaches for signal enhancement of weak acids in suppressed ion chromatography

3.1. Introduction

The identification of impurities in pharmaceuticals requires a new approach, complementary to the existing reversed-phase HPLC methods. For ionogenic analytes, the use of ion-exchange chromatography will provide orthogonal selectivity due to the different separation mechanism. However, most pharmaceutical compounds of interest are either weak organic acids or bases that have low or no UV absorbance. Moreover, a suppressed anion system produces slightly-acidic water (pH ~5.5) in which the weakly acidic analytes will be predominantly protonated and have low conductance. Since conductivity detection offers a simple and cheap alternative universal detection system, conductivity signal enhancement by an indirect method is necessary and approaches for this are examined here.

As explained in Chapter 1, introduction of a slightly basic reagent stream into the suppressed eluent carrying an acidic analyte, would yield an acid-base reaction, as described in Equation 1.18. Since the equivalent conductance of hydroxide in the reagent stream is higher than that of the analyte anion, the analyte would be detected by the equimolar replacement of hydroxide, showing decreased conductivity (negative peaks), as detailed in Equation 1.19. Base-introduction for conductivity signal enhancement has been successfully demonstrated for inorganic ions and small organic ions using home-made PCR (post-column reaction) devices [1-5], or for high concentrations of inorganic ions using a commercially-available micromembrane suppressor [6,7]. In this chapter, the potential of this approach for conductivity signal enhancement is first assessed fundamentally, by *in-situ* reaction between an eluent containing a very low hydroxide concentration (pH ~10) and a few acidic analytes of varying pK_a. Two different approaches for base-introduction are examined, the first

utilising commercially-available membrane suppressors, and the second using a simple 3-port tee-connector.

Potentiometric and pH detection have been applied for analysis of a range of inorganic acids and small organic acids in different modes of IC [8-12], however, it has not been established as a common practice. Here, in-line pH detection was performed following suppression of the eluent, using an open flow cell with a pH micro-probe. Finally, pH signal intensity either after suppression or base-introduction was compared with standard and signal-enhanced conductivity, highlighting the limitations of the two techniques and signal enhancement methods.

3.2. Experimental

3.2.1. Instrumentation

The IC system is as described in Chapter 2. Injection loop volumes of 10 µL, 25 µL, 50 µL and 100 µL were used throughout the study. Conductivity detection was also performed using a Waters-430 detector (Waters Corporation, Milford, MA, USA), connected to the data acquisition system through a Dionex UI-20 universal interface. Direct spectrophotometry was conducted using a fixed wavelength absorbance detector (Dionex AD25). pH detection was conducted with an Activon 210 pH meter (Pennant Hills, Australia) fitted with a semi-micro glass-calomel pH probe (Biolab AEP 341; Biolab, Scoresby, Vic, Australia). The pH probe interface with the eluent was via an improvised cell, as shown in Figure 3.1. In this arrangement, the outlet of the eluent coil was connected to a union fitting maintained in an upright position with a clamp. The pH electrode was placed inside (allowing free flow around the periphery of the bulb) and held stationary with a clamp. A thermocouple connected to the pH meter was dipped in a small container into which the effluent was “dripping” from the pH probe, to compensate for minor temperature changes. The pH data were transferred from the pH meter via a Dionex UI-20 to the Chromeleon® data acquisition system. Two-point calibration of the pH electrode was conducted daily off-line, using buffers at pH 4.0 and 7.0 for the suppressed system and buffers at pH 7.0 and 10.0 for the base-introduction system.

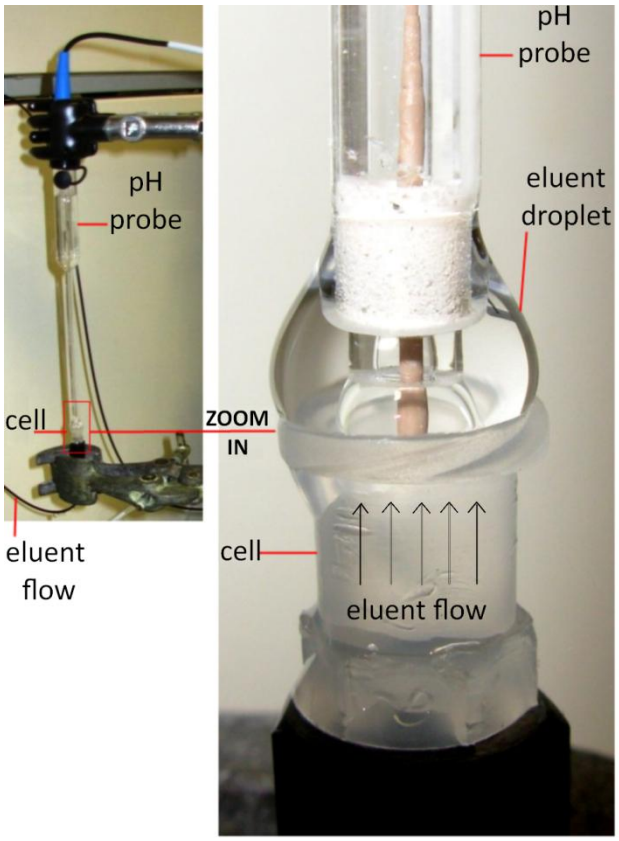

Figure 3.1 Setup of pH probe interface.

Preliminary assessment of the signal-enhancement reaction in the flow-injection mode was conducted using the system depicted in Figure 3.2. The DP pump 1 flow-rate was 0.25 mL/min flowing through the EluGen® producing 0.25 to 0.50 mM KOH. This flow was diluted by 2.25 mL/min of water from DP pump 2 joined at a 3-port tee-piece connector (Upchurch Scientific, Oak Harbor, WA, USA) before the injector, to give a KOH baseline concentration of about 100 µM. Fluctuations in flow were stabilised by a Dionex IonPac® NS1 polymeric column (250 x 4 mm) placed before the injector, acting as a pump-pulsation dampener. A number of devices were examined for the mixing of the injected acid with the alkaline flow, including a GM-4 (2 mm) gradient mixer, a GM-3 (4 mm) gradient mixer, a 375 µL knitted reaction coil and a 750 µL knitted reaction coil, all from Dionex. A conductivity detector was placed after the mixing device.

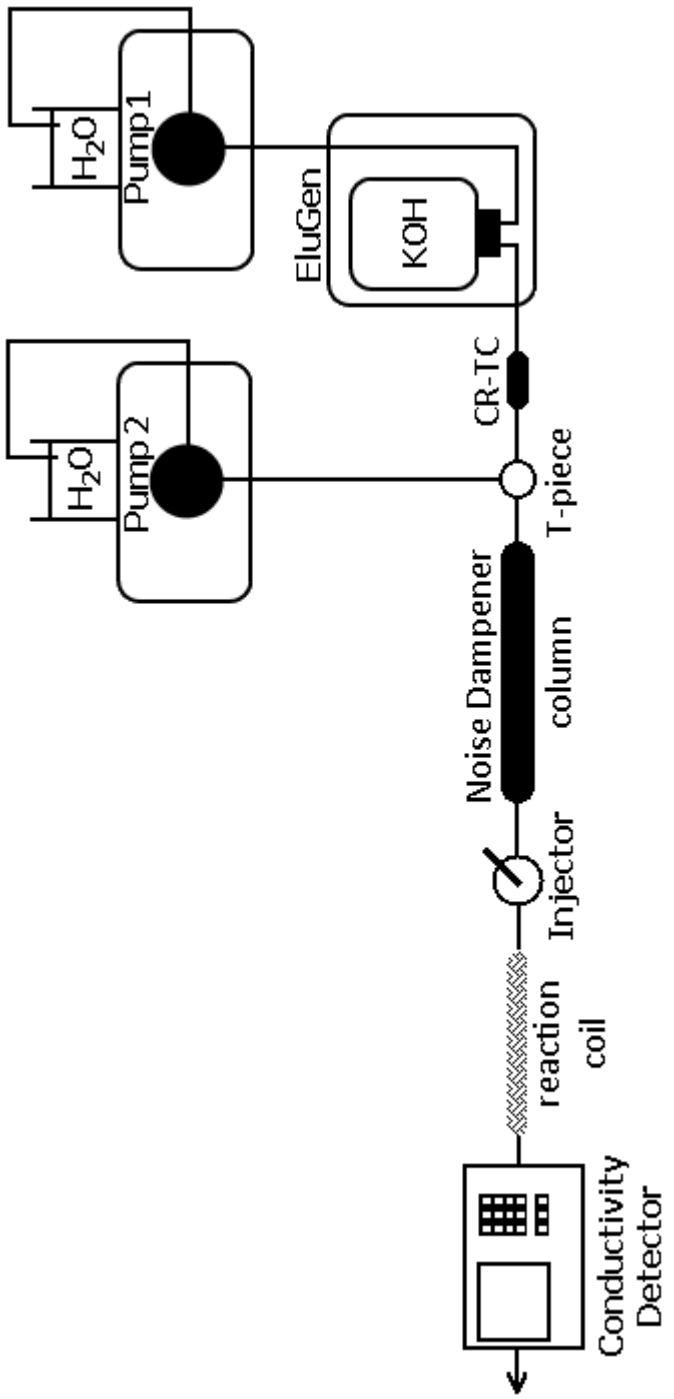

Figure 3.2 Schematic diagram of experimental system setup for acid-base reaction *in-situ*.

The instrumental configuration for calibration of base-introduction through a membrane suppressor is detailed in Figure 3.3. Water (1 mL/min) was supplied by DP pumps 1 and 2, and the 0.5-100 mM KOH was prepared using the EluGen unit connected to pump 1. The KOH solution was then introduced to the main eluent stream through a Dionex anion micromembrane suppressor (AMMS-II or AMMS-III) or an anion Atlas electrolytic suppressor (AAES), followed by conductivity detection. Aliquots of eluent were collected for off-line pH measurement once the baseline was stabilised.

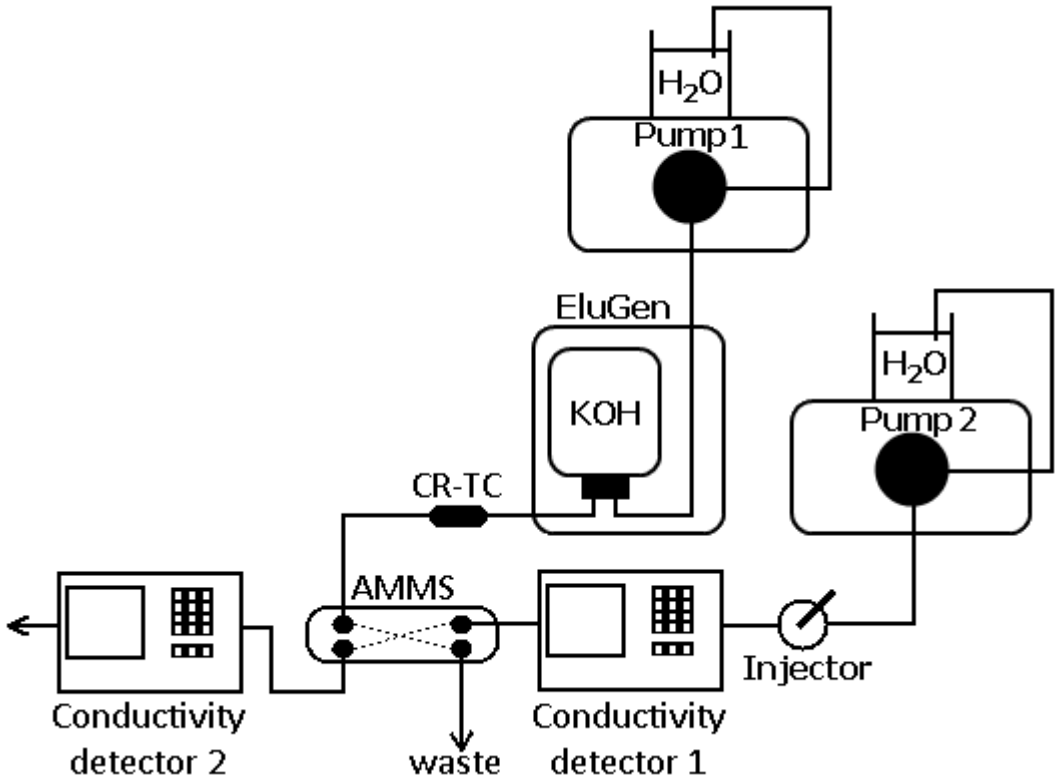

Figure 3.3 System setup for calibration of base-introduction through suppressors.

The full anion-separation system with or without base-introduction is illustrated in Figure 3.4. DP pump 1 delivered water at 1 mL/min to the EluGen unit. Eluent containing organic solvent was produced by introducing methanol after the EluGen unit [13] through a 3-port tee-connector, using pump 3 (port A), followed by a gradient mixer (Dionex GM-3, 4mm). Separations were performed using the Dionex anion exchange analytical column IonPac® AS-11 (250 x 4 mm) with a matching guard column AG-11 (50 x 4 mm), under the conditions as detailed for each experiment. DP pump 2 was the source of external water supplied at 3 mL/min for the electrolytic eluent suppressor ASRS ULTRA II® or ASRS-300® (4 mm). For base introduction, pump 4 (Jasco PU-2089i; Easton, MD, USA) was utilised after suppression, through either AMMS or a 3-port tee-connector. For base-introduction through the AMMS suppressor, a pre-made solution of KOH or NaOH at concentrations of 10-100 mM was delivered at 1 mL/min. For base-introduction through a T piece, pump 4 delivered the pre-made solution of KOH to be mixed with the eluent stream, at a flow ratio to suit the dilution factor and result in a total flow-rate of 1 mL/min. A conductivity detector, UV detector or pH meter was placed at the required position following the suppressed system. Calibration curves for suppressed conductivity and pH detection were prepared for 50 µL samples, at 5 concentrations ranging from 5 µM to 100 µM. Limits of detection (LOD) were obtained by solving the regression equation at S/N=3, unless the recorded peak height was already below the lowest limit of quantification (LLOQ, S/N=10).

3.2.2. Materials

Aqueous solutions were prepared with Ultra-pure 18.2 MΩ Milli-Q water filtered through a 0.20 µm filter (Millipore; Bedford, MA, USA). Solvents were filtered through Millipore 0.22 µm nylon filters and degassed before use. All standard stocks were stored in glass vials in 4°C prior to use. Sodium hydroxide and potassium hydroxide solutions were prepared daily from pellets (semiconductor-grade). Acetic acid hexanesulfonic acid standards were prepared by dilution with water. Other analyte solutions were prepared in 1 mM KOH in the eluent matrix (aqueous or 25% (v/v) methanol) and further diluted to make 5-200 µM standards. Relevant physico-chemical properties of the detected analytes are presented in Table 3.1.

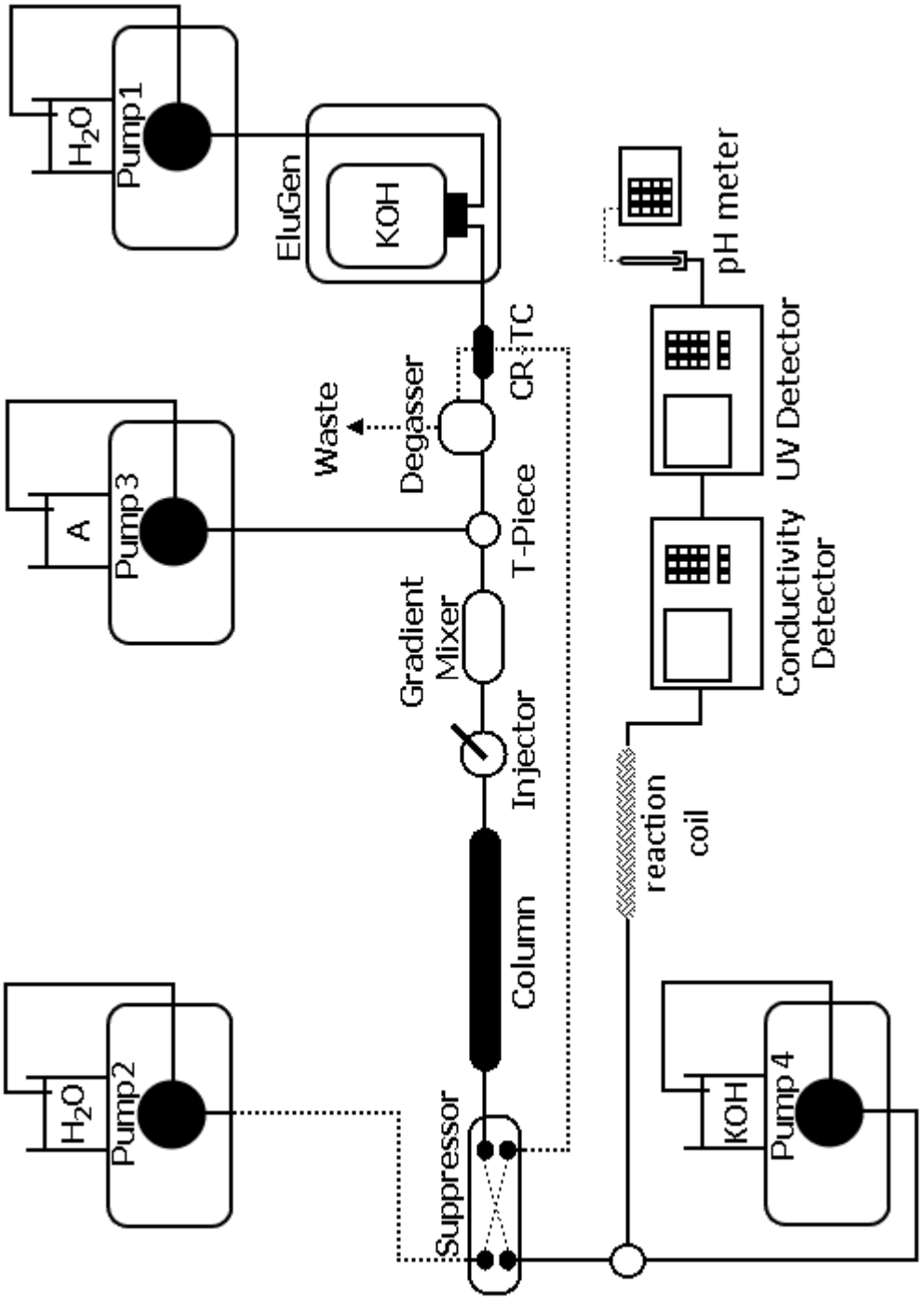

Figure 3.4 System configuration in separation mode, with conductivity, UV and pH detection. Addition of organic solvent is optional.

Table 3.1 Test set of analytes examined in this work. All data were calculated by ACD/Labs, or taken from references included in ACD/Labs v.12.00 (Advanced Chemistry Development Inc, Toronto, Canada), unless mentioned otherwise.

Analyte	MW (g/mol)	Relevant pK_a	Fractional molecular charge at pH 5.2	Fractional molecular charge at pH 10	Limiting equivalent ionic conductance ($S \cdot cm^2 \cdot equiv^{-1}$) [14]
Acetic acid	60.1	4.79	-0.6	-1	41
Carbonate	61.0	6.38	-0.86	-1.33	45
		10.32			
Boric acid	61.8	8.91	0	-0.9	26 [15]
		>14			
Succinic acid	118.1	4.24	-1.20	-2	43
		5.52			
Phenylacetic acid	136.2	4.30	-0.26	-1	29
Hexanesulfonic acid	166.2	1.99	-1	-1	27

3.3. Results and discussion

3.3.1. Conductivity enhancement via base-introduction

3.3.1.1. In-situ acid-base reaction

The potential of the use of acid-base reactions as a method for conductivity signal enhancement was first assessed in a simple flow injection system (Figure 3.2). In this arrangement, the conductivity response is governed by the extent of reaction between the injected acidic analyte and the stream of low-concentration base reagent. Hence, it was essential to achieve good mixing, while maintaining minimal sample dispersion. Mixing components and injection loop sizes were compared with the resulting peak profile. Peak shape was assessed through measurement of peak asymmetry, where non-Gaussian or W-shaped peaks indicated incomplete mixing and/or overloading, as described previously by Sjögren and Dasgupta [3]. Such effects at high analyte concentration were observed for hexanesulfonic acid, but only marginally for acetic acid and were absent for boric acid, as it depends on both the pK_a and the concentration of the reacting acid [4]. The most successful system configuration in terms of mixing and dispersion combined a 750 µL knitted reaction coil with a 25 µL sample loop, which was the highest injection volume that gave Gaussian peaks in the flow-injection mode.

After establishing a mixing system that enabled complete mixing, a range of analyte and reagent concentrations were tested, and the results were compared to theoretical values calculated by assuming complete reaction leading to full dissociation of the analyte acid. First, the molar amount of both analyte and eluent within the reaction band was calculated, based on the injected volume and the recorded peak width. Those values were then applied to an equi-molar acid-base reaction [16], calculating the concentration of the species remaining in the reaction band. The expected conductance of the reaction band was determined by substituting the concentrations and limiting equivalent ionic conductances of the species into Equation 3.1 [14]:

$$G_{\text{total}} = \frac{(\lambda_{E^+} + \lambda_{E^-})\cdot C_E + (\lambda_{E^+} + \lambda_{A^-})\cdot C_A}{10^3 \cdot K} \quad (3.1)$$

where λ is the limiting equivalent ionic conductance of the eluent anion (λ_{E^-} = 198 S·cm^2·equiv^{-1} for hydroxide), eluent cation (λ_{E^+} = 74 S·cm^2·equiv^{-1} for potassium and 50 for sodium), and analyte anion (λ_{A^-} , values in Table 3.1) [14]. C_E and C_A are the total concentrations of the eluent and the analyte ionic species, respectively, expressed as equiv·1000 cm^{-3}. *K* is the conductivity cell constant, determined for the specific detector through performing calibration (*K*=0.937 cm^{-1} for the system under study). The calculated *G* value from Eq. 3.1 was subtracted from the eluent baseline conductivity as recorded by the detector, to give the height of the recorded negative peak. The total area of the rectangular-shaped band was then obtained by multiplying the height by the peak width measured at 4.4% height. The calculated band area could then be compared to the peak area recorded experimentally. For comparison of the peak height, the reaction band was adjusted to give a Gaussian peak shape, substituting the obtained band area and width (5σ measured at 4.4% height) into the Gaussian peak equation:

$$\text{peak height} = \frac{\text{Area}}{\sigma\sqrt{2\pi}} \quad (3.2)$$

Figure 3.5 illustrates the response obtained for a range of hexanesulfonic acid concentrations in 100 µM KOH. For weaker acids (boric acid and acetic acid, pK_a >4.2) which were only partly dissociated in the suppressed eluent, full dissociation was expected in the applied base concentration (100 µM, pH 10), according to the data presented in Table 3.1. The low sample concentrations used in this set of experiments could further contribute to analyte dissociation, overcoming the decrease in conversion rate with increasing pK_a [1]. At a hexanesulfonate (HSA) concentration of 250 µM and more distinctly at 1 mM, the asymmetrical peak shape indicates incomplete mixing. For a range of analyte concentrations (10-125 µM), the observed responses for the three examined acids were very close to each other, with boric acid showing a response lower only by 10-20% compared to that observed for hexanesulfonate. However, the similarity between the acetic acid and the hexanesulfonate responses was not consistent with that expected according to their limiting equivalent ionic conductances. The limiting equivalent ionic conductance of acetate is almost double than that of hexanesulfonate, hence the higher conductance at the peak maximum of acetic acid should theoretically lead to a smaller negative peak.

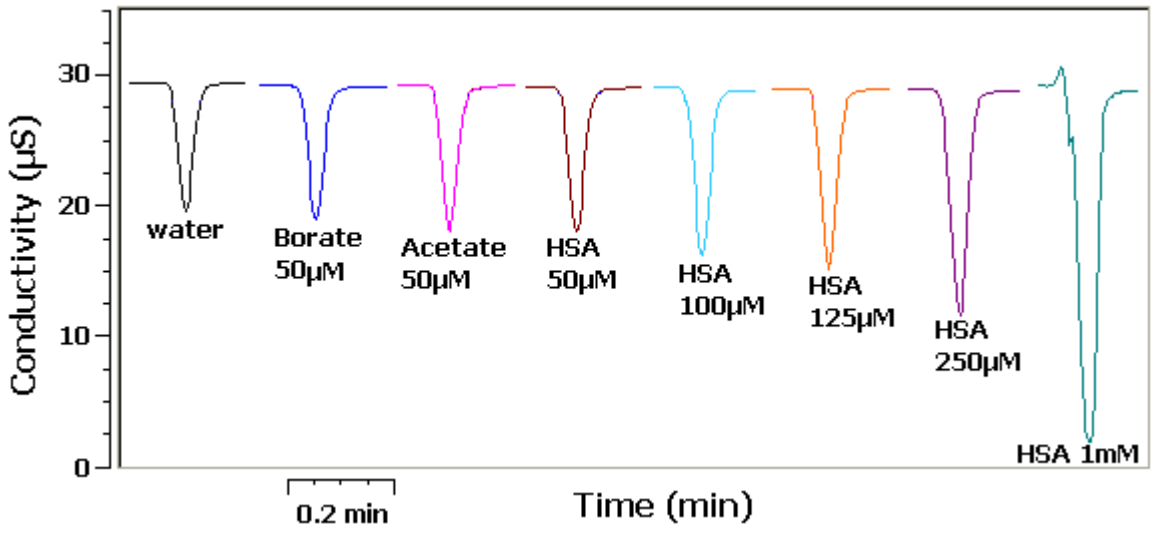

Figure 3.5 Conductivity results from *in-situ* reaction between 100 µM KOH eluent and 25 µL injected samples (HSA = Hexanesulfonic acid). The system configuration is detailed in Figure 3.2. A total flow-rate of 2.5 mL/min was applied, and a 750 µL knitted reaction coil was used for mixing after injection.

Figure 3.6 summarises the peak data for hexanesulfonic acid presented in Figure 3.5, indicating that at concentrations below 250 µM the experimental peak was similar to the predicted result, with only a 0.5% - 2% difference for peak area, and 0% - 7% difference in peak height, supporting the feasibility of this approach and defining its limitations.

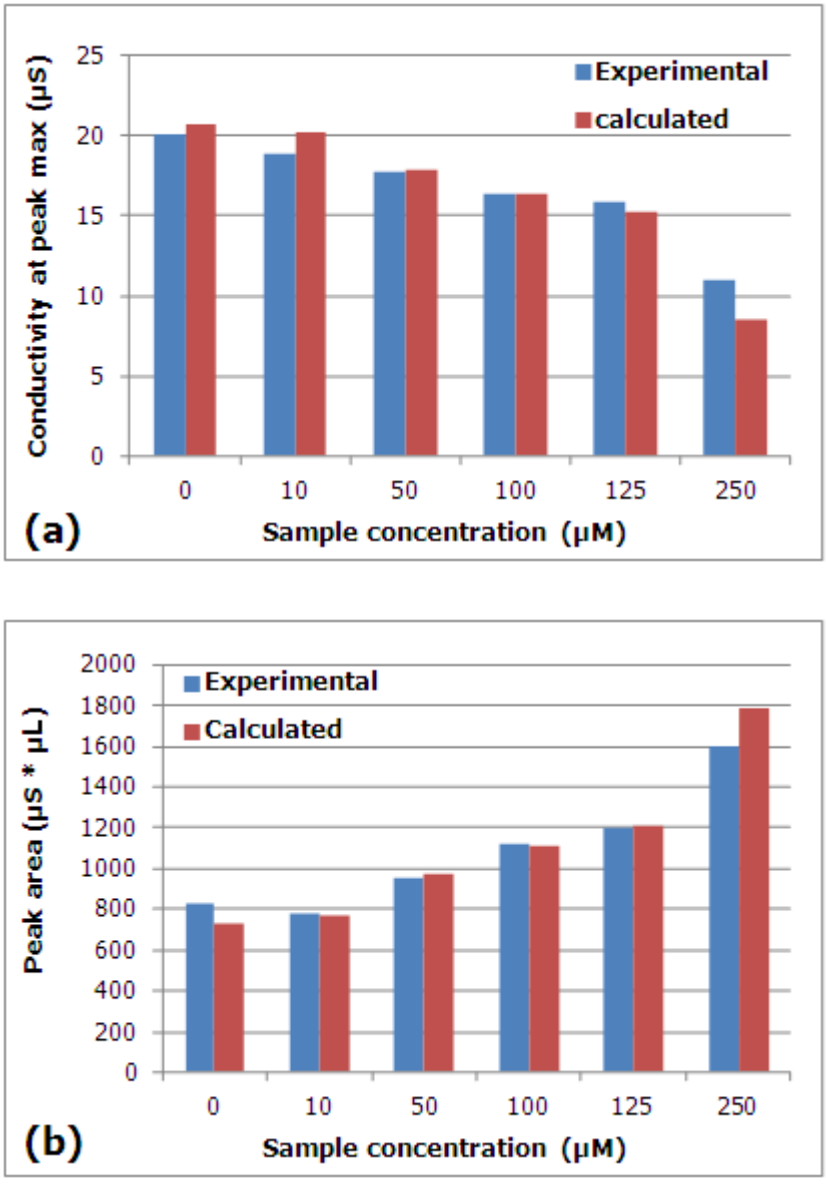

Figure 3.6 Comparison between experimental and calculated conductivity values for peak maxima (a) and peak area (b), of 25 µL hexanesulfonic acid injected into 2.5 mL/min 100 µM KOH eluent system described in Figure 3.2.

3.3.1.2. Base-introduction via a micromembrane suppressor

This approach for signal enhancement via a post-suppression acid-base reaction involved the re-introduction of base into the eluent stream through a membrane suppressor using a hydroxide solution in the regenerant chambers. The capability of commercially-available membrane suppressors for this purpose was evaluated using a flow-injection system (Figure 3.3). The applied base concentration had to be sufficiently high to overcome the Donnan exclusion effect of the cation-exchange membranes in the suppressor, yet not to exceed an applicable conductivity level. Passive Donnan membrane "leakage" through the suppressor was calibrated for a wide concentration range of sodium hydroxide (pre-made) and potassium hydroxide (EluGen prepared). The concentrations of the introduced base were calculated from the recorded conductance *G* employing Equation 1.4. The accuracy of the calculated concentration ($C_{E\ (mM)}$) was also confirmed by off-line pH measurements, using Equation 3.3:

$$pH = 14 - \log(10^{-3} C_E) \qquad (3.3)$$

Equal amounts of hydroxide permeated through the membranes of the Dionex AMMS II suppressor from either KOH or NaOH feed solutions. The Dionex AMMS III suppressor showed very low penetration levels (≤0.1% of the feed concentration) compared to ≤1.2% for the AMMS II suppressor (Fig. 3.7). The effect of the age of the specific suppressor unit was not examined here, although elevated penetration rates were expected for an older unit, as reported previously [6]. The Dionex anion Atlas suppressor (AAES), which consists of ion-exchange monoliths and membranes in flow-distribution discs, did not allow any leakage even at very high regenerant concentrations (100 mM) over a period of 4 hours. The hydroxide introduction rates through the AMMS suppressors were similar to those shown for tubular Nafion membrane devices designed and fabricated by Dasgupta and co-workers [1,5]. Yet, while these home-made devices resulted in improved conductivity signals for some inorganic and organic ions, use of commercial suppressors in our work did not lead to any significant signal enhancement.

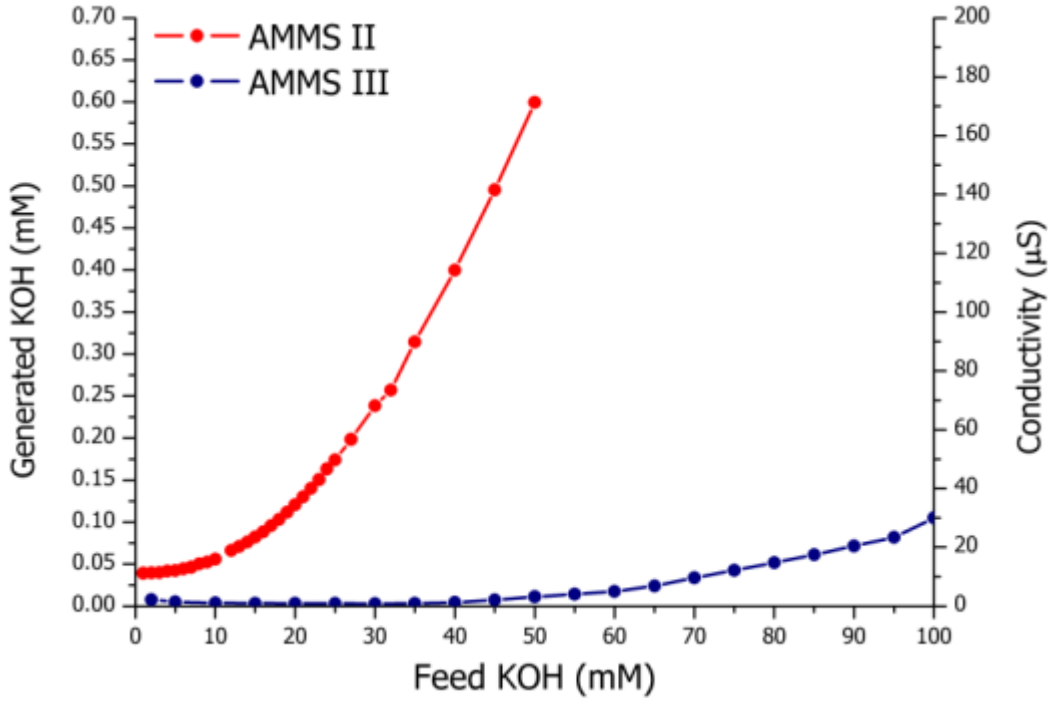

Figure 3.7 Correlation between the feed KOH concentration made by EluGen, and the generated KOH (left Y axis) and conductivity (right Y axis), in the AMMS II suppressor (red dots) and the AMMS III suppressor (blue dots), using the system configuration in Figure 3.3.

For either strong or weak acids (hexanesulfonic and acetic acids) the typical negative peaks and W-shaped peaks in case of analyte overload, were observed (Figure 3.8), but without any improvement compared to the conductivity detection prior to base introduction. Peak dispersion caused by the suppressor (which typically has an internal void volume of 50 µL) could not be used to explain the poor conductivity response. Inadequate mixing between the analyte and the base was also ruled out, since the use of a high volume mixing coil after the suppressor resulted in retention time shifting yet without any change in peak shape, height or area. A possible reason for lack of signal enhancement following base-introduction through commercial membrane suppressors may lie in precipitation or adsorption of the analyte onto the suppressor membrane by hydrophobic or ionic mechanisms, as demonstrated later in Chapter 5. A suppressor with a neutral screen (low ion-exchange capacity) can aid in the mechanism of leakage, yet would cause high peak dispersion due to adsorption effects [17].

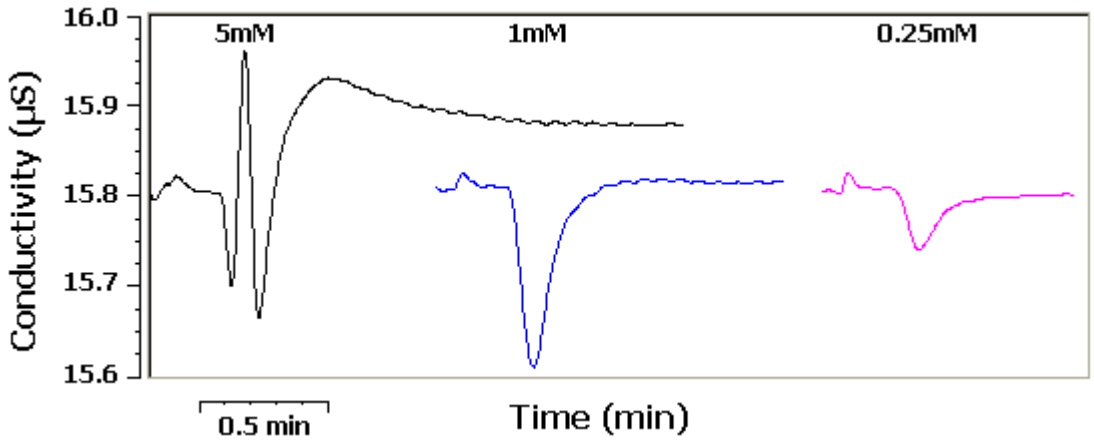

Figure 3.8 Negative conductivity peaks of 10 µL injected acetic acid at different concentrations as indicated above each peak, after introduction of approximately 60 µM KOH through the AMMS-III suppressor. The system configuration is detailed in Figure 3.4.

Additionally, insufficient reaction rates can be caused by the laminar flow pattern along the suppressor membrane, which results from the base-introduction, due to the steep gradient from 100 mM KOH on the regenerant side of the membrane to 100 µM on the eluent side [17]. Caliamanis and co-workers [6] encountered a problem while introducing hydroxide via a commercial membrane suppressor, which was described as uncontrolled leakage of the base regenerant through the membrane. Dasgupta *et al.* [5] explained that the commercially-available membrane suppressors are not ideal for passive base-introduction due to their suppression-focused design. Firstly, there might be a decrease in the concentration of the penetrating base, presumably by ion-exchange processes on the screens of the regenerant chamber, in addition to those on the membranes. On top of the desired ion-replacement of analyte hydrogen by the introduced cation on the suppressor membrane, ion-exchange interactions can occur on the screens of the suppressor eluent chamber. If the acid analyte is significantly ionised, its hydrogen ion can be exchanged for a metal cation on the screen, as well as on the interior membrane surface. The regeneration of the ion-exchange sites on the screens is slower than on the membranes, therefore until a change in baseline occurs, a positive peak for the formed salt will be present on top of the background of the introduced base, where a negative peak is expected. This effect simply differentiates strong acids (positive peaks) from weak acids (negative peaks).

The unsuccessful results in this approach led to the evaluation of a second method of base-introduction.

3.3.1.3. Base-introduction through a tee-connector

A simpler method for post-suppressor base-introduction is via a 3-port tee-connector, combining the suppressed eluent flow with a base reagent stream, followed by a low-dispersion mixing coil. Although expected to cause some peak broadening and background noise due to mixing in the tee-connector, this approach avoids the complications of unknown interactions in the micromembrane suppressor.

This system was first evaluated for the degree of mixing and reaction according to peak height and asymmetry, leading to the use of a large volume injection (100 µL). An accurate predictability of the conductivity signal was established via a method for quantification of acid-base reaction in non-Gaussian peaks for a strong acid (hexanesulfonic acid). The concentration of the analyte at the peak maximum was calculated using Equation 3.4 from the peak height (*h*) obtained by direct conductivity measurement after the introduction of water:

$$C_{A\ \text{peak max}} = \frac{h \cdot K}{(\lambda_{E+} + \lambda_{A-}) \cdot 10^3} \qquad (3.4)$$

where λ_{E^+} is the limiting equivalent ionic conductance of H^+ and λ_{A^-} is the value for the analyte anion (Table 3.1). This resulting concentration (in mM units) reflects the dispersion and dilution of the peak by the base-introduction stream. The calculated concentration value was assumed to react in an equi-molar mode with the introduced base (without changing the peak shape dramatically), yielding baseline conductivity relative to the difference between the limiting equivalent ionic conductance of hydroxide and the limiting equivalent ionic conductance of the analyte anion. The calculation was made by substitution of the calculated concentration into Equation 1.6, which calculates the change in conductivity [14]. For example, chromatogram 1 in Figure 3.9 illustrates the conductivity response of a 25 µL sample of 100 µM HSA. According to the peak maximum received in the conductivity detector after water introduction (a), the concentration at that point was 70 µM HSA. Applying this value to the peak maximum after base-introduction (b) gives an expected peak height of 12.7 µS, which is, once adjusted for the negative change in conductivity, deviated by only 5% from the experimental conductivity change.

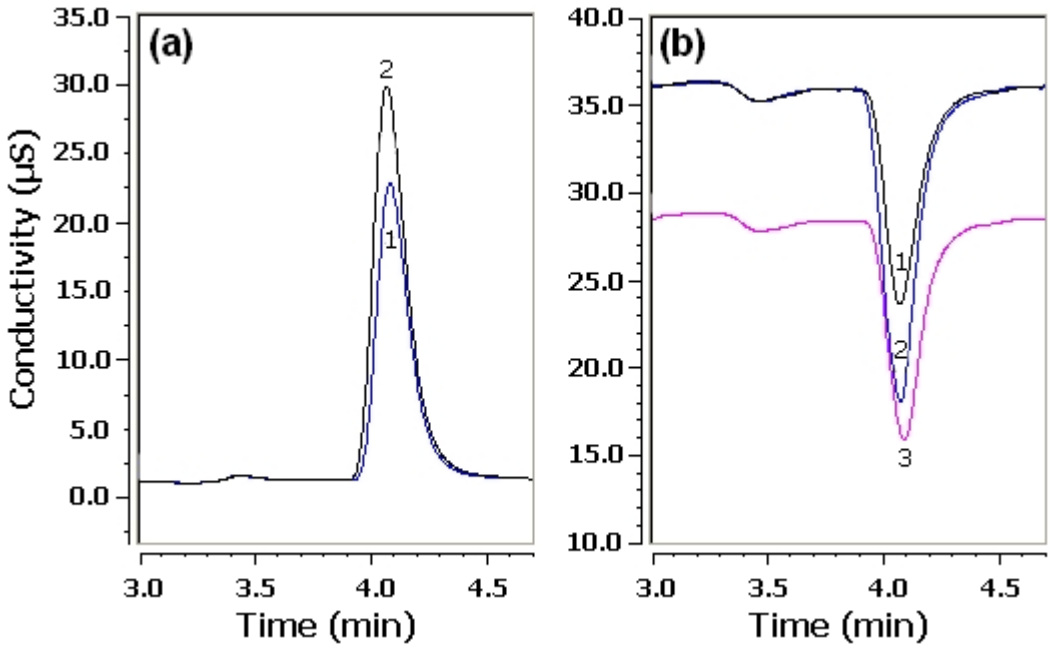

Figure 3.9 Conductivity of 25 µL hexanesulfonic acid 100 µM (1,3) or 125 µM (2) separated on an AS-11 column by 50 mM KOH, after water introduction (a) and after base-introduction (b), where two levels of base were introduced, resulting in baseline levels of 125 µM KOH (blue and black baselines) and 95 µM KOH (pink baseline).

Figure 3.9 also demonstrates how the amount of introduced hydroxide has a low degree of effect on the reaction rate, as long as it is not the limiting factor of the reaction (insufficient to fully neutralise the acidic analyte). The overall comparison between the experimental and calculated conductivity showed a high degree of correlation, with a maximum of 10% difference, presumably due to excess hydrogen ions which remained in the system after suppression and were available for reaction.

The introduction of water as a calibration method for peak values after base introduction, owing to the exclusion of dispersion influence, also enabled more accurate assessment of the conductivity signal enhancement of weaker acids. Figure 3.10 shows that base-introduction indeed has a potential for conductivity signal enhancement of weak acids. Conversion of partially ionised weak acids to fully dissociated species could increase the conductance despite the lower limiting equivalent ionic conductance of K^+ (74 $S \cdot cm^2 \cdot equiv^{-1}$) compared to H^+ (350 $S \cdot cm^2 \cdot equiv^{-1}$).

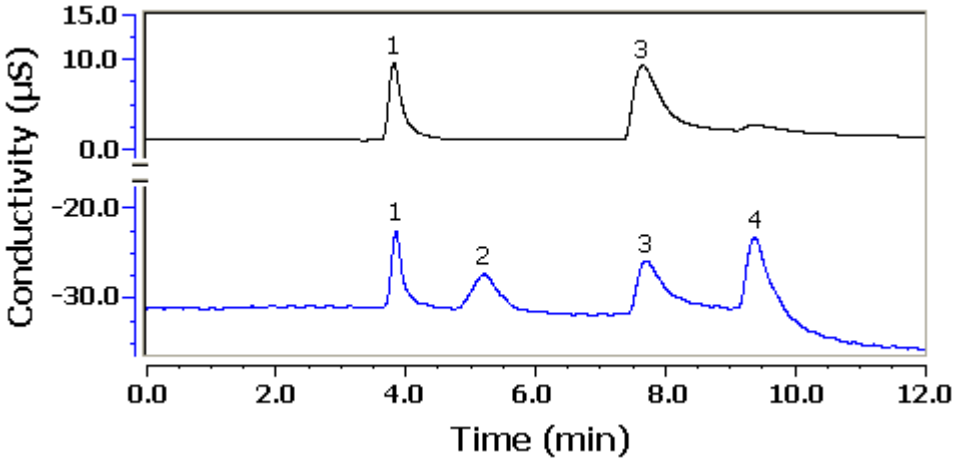

Figure 3.10 Separation of 100 µL multicomponent sample containing 200 µM of each analyte, on an AS-11 column by a linear ramp from 3 mM to 18 mM KOH starting at 3 min. Peak identities: acetic acid (1); boric acid (2); phenylacetic acid (3); carbonate contamination (4). The top channel is suppressed conductivity detection after introduction of water, and the bottom channel is the mirrored chromatogram recorded after base introduction. The flow-rate ratio between the main eluent flow and the introduced base stream was 0.75:0.25 mL/min. The system configuration is detailed in Figure 3.4, without the addition of organic solvent.

As expected for stronger acids which are fully dissociated at low pH, the conversion from the protonated form would always result in decreased conductivity. For weak acids, though, signal enhancement was observed only at high volumes and concentrations (>100 µM). This behaviour was also observed by Caliamanis *et al*. [18] and was found to be related to a "critical concentration point" of the analyte ("CPC"). Below a certain concentration, the dissociation of a weak acid is improved despite the pH of the eluent. Only at higher concentrations where the ionisation of low-pK_a analytes is decreased [19], does their conversion from HX to K^+X^- actually becomes beneficial despite the large difference in the conductance between H^+ and K^+. Another reason for lack of enhancement for weak acids at lower concentrations was the analyte plug dilution due to mixing with the reagent, bringing the concentration of some analytes to below the low limit of quantification (S/N=10) after base introduction. The magnitude of enhancement observed in Figure 3.10 was quantified as the ratio of peak height between water introduction and base introduction. As Figure 3.11 illustrates, the ratio calculated for the four analytes was found to be inversely proportional to the analyte pK_a. According to this plot, analyte pK_a of about 4.5 appears to be the critical value for conductivity enhancement for introduction of base of pH ~10.

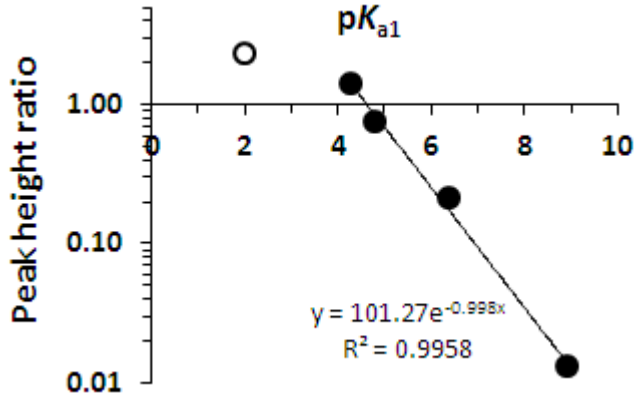

Figure 3.11 Conductivity peak height ratio (water-introduced / base-introduced) on a logarithmic scale, as a function of analyte pK_a. For suppressed conductivity of boric acid (the lowest data point), the results for 1 mM sample were used since 200 µM was below limit of detection. Hexanesulfonic acid (the highest data point, open circle, 100 µM) was not included in the regression line. Conditions are detailed in Figure 3.10.

In the suppressed eluent, where the pH is about 5.2-5.5, analytes with these pK_a values would experience partial dissociation, for example acetic acid, pK_a 4.7, would be about 40% protonated at pH 5.2 (see Table 3.1).

When the base-introduced response was compared directly to the suppressed conductivity (without the exclusion of the dilution effect caused by reagent mixing at various ratios), the enhancement factors were much lower, as expected. The extent of peak dispersion caused by dilution while mixing with the reagent would be reflected in the peak height in the second conductivity detector, yet in some cases the peak area in this detector was found to be higher. Figure 3.12 illustrates the differences in response after base-introduction for various sample volumes. Higher sample volumes presented increased peak height ratio between the base-introduced conductivity signal (CD2) and the suppressed conductivity signal (CD1). The boric acid enhancement factor could not be calculated due to lack of response after suppression at concentrations lower than 1 mM, as reported before for suppressed conductivity detection [2,3,5,20]. The reason for the difference in enhancement factors seems to originate not only in higher rates of acid-base reactions but was also related to a non-linear decaying increase in suppressed conductivity response at larger volumes (and total amounts). After suppression, the peak heights were logarithmically related to the sample volume (r^2 >0.99), which is a known attribute of suppressed conductivity detection of samples in high amounts, due

to changes in dissociation levels [19]. After base-introduction, the peak heights and areas were linearly related to the sample volume (r^2 >0.995 for peak height and r^2 >0.999 for peak area) however the peak height and area for 25 µL samples were 4 times smaller than those from 50 µL samples, which were half the 100 µL samples. This, again, demonstrates the inferior enhancement achieved at lower sample volumes, which has also been detailed by Fotsing *et al*. who chose 500 µL injections for their post-column reaction after suppressed conductivity [21].

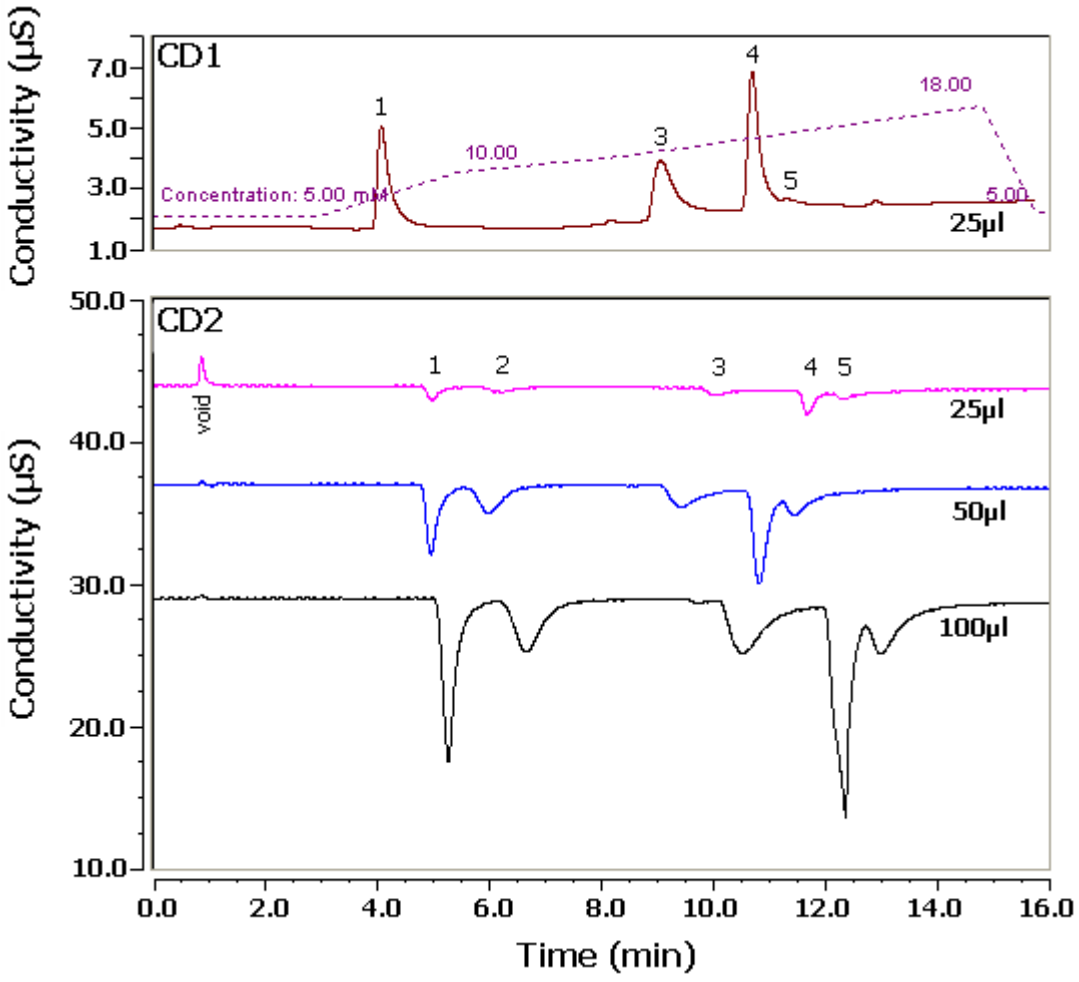

Figure 3.12 Two-channel chromatogram of 200 µM multicomponent sample, with injection volumes as indicated under each chromatogram. Suppressed conductivity (CD1) is the top channel, followed by base-introduction (CD2) achieving approximately 100 µM KOH baseline. The 50 µL and 25 µL chromatograms were shifted to fit the retention times of the 100 µL sample, and also shifted in the signal axis from a uniform 29 µS baseline. 0.5 mL/min main eluent flow was introduced with a base reagent flow at 0.5 mL/min. Peak identities: acetic acid (1); boric acid (2); phenylacetic acid (3); succinic acid (4); carbonate contamination (5). The aqueous KOH multi-step gradient is detailed in the broken line in the CD1 chromatogram. The system setup is as detailed in Fig. 3.4 without the addition of organic solvent.

The ratio of mobile phase flow-rates mixed in the tee-connector affected the enhancement factor in a manner proportional to the dilution. Its effect on peak height is of great importance because of the high noise levels observed after base-introduction (50-75 nS), compared to the noise level in a suppressed system (1 nS). This noise is caused by mixing and mainly by pulsation from the pump introducing the base, and has been observed in a range of post-column reaction devices [22]. The low signal-to-noise values presented in Table 3.2 demonstrate the drawback of the enhancement method, adding to the limitation that enhancement is only efficient at high analyte concentrations. Fotsing *et al.* [21] have optimised the electrolytic suppression before PCR and the mixing ratios with the introduced reagent, and achieved the highest peaks on the first dimension while applying 1 mL/min eluent flow, above which lower column efficiency was observed under the separation conditions.

Amendment of the ionic eluent with organic solvent is essential for analysis of hydrophobic pharmaceuticals, particularly during suppression when the eluent hydroxide is eliminated and the pH drops. For example, mefenamic acid, which has a log *P* above 5, is immiscible in water despite having a pK_a below 4.3, but is soluble in alkaline hydroxide solutions (0.5 ppm at pH 5; 100 ppm at pH 7.4 [23]). Hence, after suppression it would be prone to precipitation. However, the dielectric constant of the ionic eluent containing organic solvent is lower compared to an aqueous eluent, and this increase in eluent resistance would result in reduced analyte conductivity levels [24]. Weak ions will be more affected, and will show lower dissociation than in water. For example, the dissociation constant of acetic acid is 4.9 at ~13% (v/v) methanol and 5.27 at ~40% (v/v) methanol [25].

When the conductivity experiment was repeated using eluents containing 25% (v/v) methanol, the magnitude of enhancement was maintained or even improved. As Table 3.2 details, it was not necessarily the quality of the acid-base reaction, but a reduction in the suppressed conductivity signal, as recorded for all analytes in varying magnitude. Apart from the effect of the solvent on the analyte dissociation level and conductivity, the signal was compromised due to an elevated (~5 µS) and noisier (5-10 nS) suppressed baseline in the presence of 25% methanol, as discussed at length in Chapter 4. These effects were reflected in a decreased signal-to-noise ratio despite improved or similar enhancement values.

Table 3.2 Conductivity peak results for a standard suppressed system (CD1) and after base-introduction (CD2), for 100 µL samples. The mixing ratio between the main eluent stream and the introduced base was 0.85 : 0.15 mL/min.

Analyte	Peak Area (µS·min)			Peak Height (µS)			S/N ratio	
	CD1	CD2	CD1/CD2	CD1	CD2	CD1/CD2	CD1	CD2
Acetic acid 200µM								
Aqueous KOH	3.57	2.80	1.27	14.70	14.92	0.99	14696	248
KOH in25% MeOH	2.25	3.03	0.83	11.14	14.84	0.75	2228	165
Boric acid 200µM								
Aqueous KOH	0.004*	2.24	0.002	0.03*	5.04	0.006	26	84
KOH in25% MeOH	n/a	1.57	n/a	n/a	3.07	n/a	n/a	34
Phenylacetic acid 200µM								
Aqueous KOH	4.22	2.19	1.93	9.45	5.22	1.81	9445	87
KOH in25% MeOH	3.91	2.88	1.36	9.11	7.30	1.25	1822	81
Carbonate (unknown)								
Aqueous KOH	0.57	3.24	0.17	1.99	8.26	0.24	1987	138
KOH in25% MeOH	0.18	3.40	0.05	0.41	6.50	0.06	82	72

* Suppressed conductivity as measured for 1 mM sample.
n/a, Suppressed signal in KOH containing 25% (v/v) MeOH was below LOD.

Also, the addition of methanol to the eluent did not prevent the peak tailing observed earlier, and it added complexity to the chromatogram due to the methanol peak eluting with the void. Nevertheless, if addition of solvent is required for analysis of the target compounds, the suppressed conductivity under those conditions should be considered the starting point for enhancement, instead of the suppressed conductivity in aqueous eluent.

Overall, the findings presented here suggest that base-introduction can be conducted via a tee-connector but not via a membrane suppressor, and efficient signal enhancement is limited to weakly-acidic analytes at high concentrations and injection volumes. This fundamental investigation of the enhancement mechanisms was challenged by the lack of a simplified set of analytes, due to a limited availability of target compounds which satisfied the experimental requirements (non-zwiterionic; preferably monoprotic acids with pK_a >4.8; soluble in aqueous eluents of pH <6). Boric acid, for example, was not an ideal compound, as it consists of a variety of species, and is prone to interact in the electrolytic suppressor prior to base introduction.

3.3.2. pH detection

3.3.2.1. Suppressed system

Another approach for signal enhancement of weak organic ions was pH detection following eluent suppression. Firstly, the system was calibrated and the pH signal validated both in value and in relative time of response. On the calibrated system, pH detection provided negative peaks following suppression of aqueous eluents under isocratic or shallow gradients, as presented in Figure 3.13. The baseline noise was identical to suppressed conductivity (0.001 mV), in a similar manner to that reported in previous comparison studies between conductivity and pH detection [10]. Under isocratic elution, the pH peak heights were superior to those recorded under gradient elution, as previously published for inorganic ions [9].

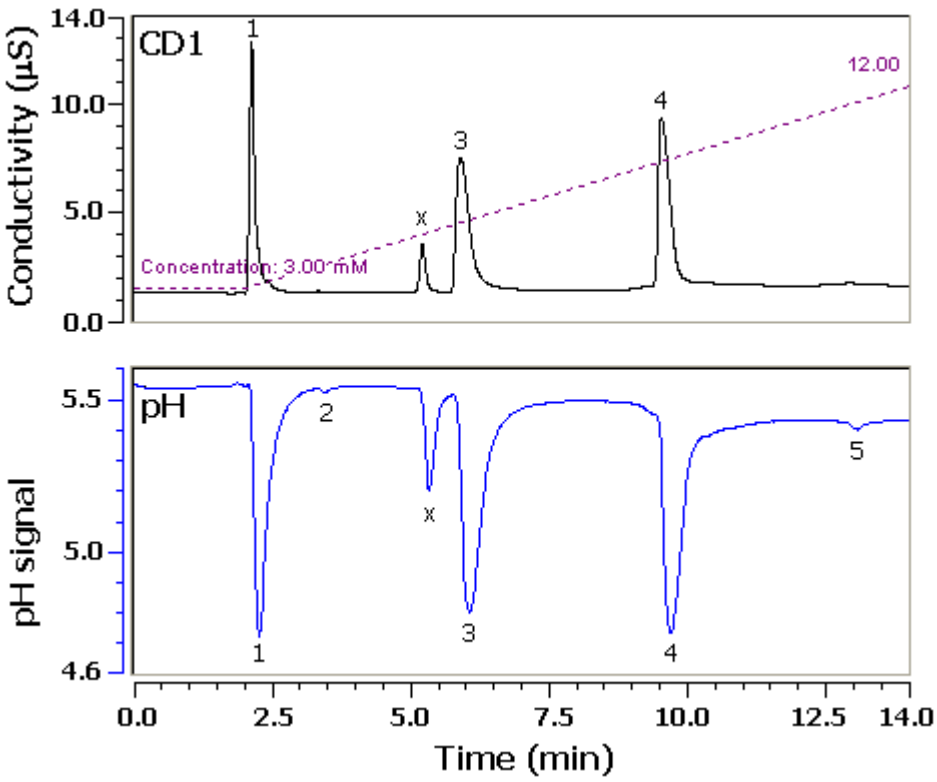

Figure 3.13 Two-channel gradient chromatogram for a 50 µL multicomponent sample, 100 µM of each analyte, with suppressed conductivity detection at the top channel (CD1) and pH detection below. Peak identities: acetic acid (1); boric acid (2); phenylacetic acid (3); succinic acid (4); carbonate comtamination (5); contamination associated with phenylacetic acid (x). A linear eluent ramp was applied, as indicated by the broken line in CD1 channel. The system configuration is detailed in Figure 3.4, without base-introduction components.

The shallow gradient from 3-12 mM KOH in 12 min resulted in some baseline drift, yet it could not account for the decreased peak height over the first half of the chromatogram. Five-point peak area calibration plots of the examined range of concentrations (5-100 µM) showed a power correlation with coefficients above 0.99. The peak heights plotted against concentration fitted the expected logarithmic regression, reflecting low response at concentrations below 25 µM, again, as reported previously for pH detection with a suppressed eluent [9]. It is possible, however, that analyte concentrations higher than 100 µM would have resulted in a linear regression model, as reported for inorganic ions [12]. Suppressed pH detection exhibited satisfactory sensitivity to analytes with pK_a values around 4, yet failed to present any improvement for weaker acids (Table 3.3). The limits of detection for the three quantified acids, calculated by solving the non-linear regression equation at S/N=3, were 2-5 µM (~1 ppm), which was identical to the range reported by Trojanowicz *et al.* for potentiometric pH detection of inorganic anions [10]. Shintani and Dasgupta detected common inorganic anions at concentrations of 25-200 µM after suppression of an anionic eluent gradient. They optimised a home-made flow cell with a flat surface pH electrode, yet the best recorded response was only slightly worse than conductivity detection, with 2 µM LOD for anions with pK_a values above 2 [9].

Table 3.3 Comparison between suppressed pH and conductivity detection (CD1) peak results for 50 µL 100 µM samples. Unless mentioned otherwise, the limit of detection (LOD) was calculated by solving the regression equation obtained for 5-100 µM samples, at S/N=3. The eluent flow-rate was 1 mL/min.

Analyte	Peak Area		S/N ratio		LOD	
	CD1	pH	CD1	pH	CD1	pH
	µS·min	mV·min			µM	µM
Acetic acid	1.36	0.25	11580	820	0.002	2.2
Boric acid	n/a	0.002	n/a	12	n/a	100*
Phenylacetic acid	1.77	0.31	6166	710	0.015	3.0
Succinic acid	1.84	0.27	7730	700	0.031	4.7
Carbonate	0.023	0.006	128	5	n/a**	n/a**

n/a, Suppressed conductivity values below limit of detection.
* No calibration plot available, hence value is based on LLOQ.
** No concentration data available (introduced contaminant only).

In the present study, despite reasonably low LODs, the response of pH detection was at best 4-times lower than suppressed conductivity, which was similar to LODs observed in the literature [10]. In the instrumental configuration used here, the lack of enhancement could be partly due to band broadening before and inside the home-made cell into which the pH probe was inserted.

3.3.2.2. Post-suppression base-introduction

pH detection was further examined after base-introduction which increases the pH of the eluent to pH 10. The pH of the analyte mixture is expected to deviate from the pH baseline proportionally to the concentration of the acidic analyte emerging from the suppressor. Figure 3.14 illustrates that pH detection after base-introduction was insensitive to low sample concentrations, even when high sample volumes were injected. Applying very high sample volumes and concentrations caused incomplete mixing with the introduced base reagent, evident by deformed, non-Gaussian peaks on the conductivity detector, yet owing to the dispersion and mixing in the pH cell, the pH signal seemed less asymmetrical than that from the conductivity detector. The impact of dilution by reagent mixing in this complex system was noticeable and was accompanied by high noise levels resulting from pump pulsations and eluent mixing. Compared to pH detection without base introduction, there was a 5-fold average decrease in peak response. This decrease did not include the diprotic succinic acid (at high concentrations), and can be explained by the average charge of succinic acid in pH 10 solution (-2) compared to pH 5.2 solution (-0.6), as summarised in Table 3.1. As for boric acid, although it was not separated from acetic acid peak under the applied gradient conditions, when the elution conditions were adjusted it was still not observed as a pH change after base introduction.

In work reporting similar principles, Egashira *et al.* [8] have designed a flow-through pH detector with a hydrogen ion selective glass electrode, for the direct measurement of carboxylic acids. The ion-exchange effluent was first modified to alkaline pH, using a post-suppressor packed column. Then, once the analytes were fully dissociated, a stream of buffer reagent was introduced, and the deviation from the original pH of the buffer solution was monitored, as this was proportional to the concentration of the analytes.

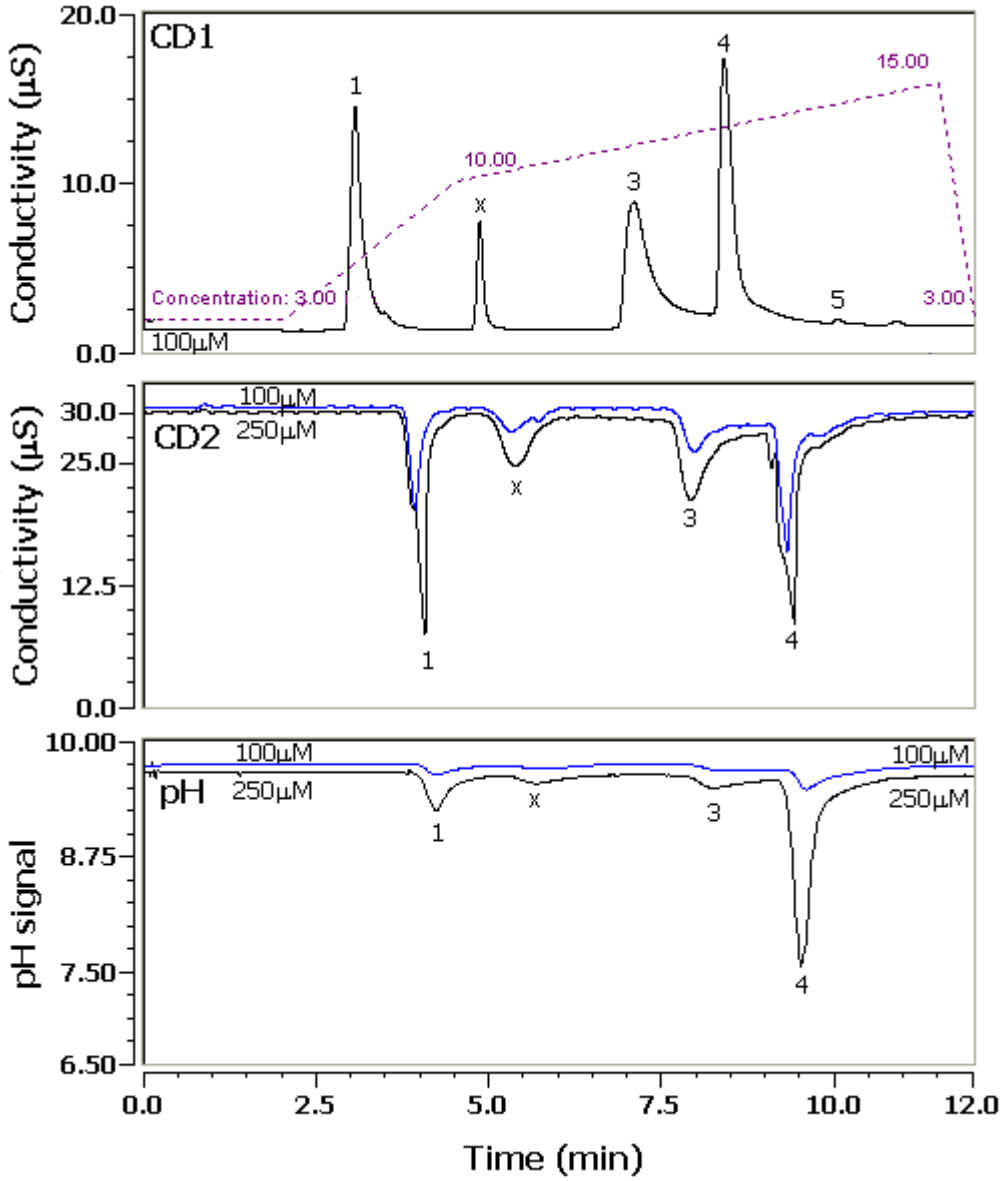

Figure 3.14 pH measurements for a 100 µL multicomponent sample at concentrations as indicated for each chromatogram: Suppressed conductivity at the top channel (CD1), followed by conductivity after base-introduction (CD2) and pH response after base-introduction at the bottom channel. Peak identity: acetic acid (1), contamination associated with phenylacetic acid (x), phenylacetic acid (3), succinate (4), carbonate contamination (5). A multi-step gradient was applied as indicated by the broken line in CD1 channel.

The change in pH for 500 µL samples of injected carboxylic acids (and also carbonate), ranged from 0.05 to 0.1 pH units, and their limits of detection were reported to be 1-10 µM. However, these findings relied on injection of very high volumes (500 µL) and analyte concentrations (10 mM), and no calibration data were presented as a basis for calculating the limits of detection.

The findings of the assay presented here mostly confirm the presumption that the pH change depends on the eluent [16], and that an acid-base reaction yields a minor change in hydroxide concentration for pH 10 eluents. This is in contrast to that observed in suppressed pH detection, where a more distinct change of pH was generated by elevation of hydrogen ion concentration in the slightly acidic pH solution. Shintani and Dasgupta [11] have also shown that pH sensitivity is highest close to neutral pH. They improved the system of suppressed-pH detection [9] through pH modification, by immersing the post-suppressor effluent tubing in ammonium solution. The pH detection sensitivity for 100 µM inorganic anions was enhanced by 2.5-fold with increasing eluent pH (which depended on the ammonium concentration), peaking at pH 6.7, and dropping dramatically in alkaline pH [11].

3.3.2.3. Compliance with application demands

In view of the application requirements, several factors would hinder the successful employment of pH detection for routine work in industry. Firstly, the repeatability of pH detection was unsatisfactory over several days, due to the impact of minor changes in the suppressed matrix at a pH close to neutral. Secondly, many pharmaceuticals, even ionogenic ones, are hydrophobic and suffer from low solubility [23], hence the addition of organic solvent at moderate concentration is frequently required. Moreover, pH detection is of limited value when applied to solutions containing organic solvents [26,27], as required in this work. Lastly, pH detection is more stable under isocratic conditions, yet complex gradients are necessary for gaining sufficient selectivity for weakly ionised pharmaceutically-related compounds on commercially-available ion-exchange columns (as detailed in Chapters 4 and 7).

3.4. Conclusions

In this chapter, two detection techniques were examined for their potential to enhance the conductivity signal of weak organic ions after suppression. The potential of the first approach, indirect conductivity signal enhancement by post-suppression reaction, was investigated by studying the mechanism of this acid-base reaction and confirming the expected decrease in the background signal. When implemented in a chromatographic system, signal enhancement was achieved using a tee-connector for

base introduction, but not by a commercially-available micromembrane suppressor. Introduction through a membrane suppressor provided a stable baseline, yet proved to be not feasible for efficient reaction with injected weak acid analytes. The former approach resulted in good enhancement of response for analytes with pK_a values above 4.7, however the resulting signal enhancement was found to be inconsistent over a series of analyte concentrations and volumes, and limited to high analyte amounts. Due to high background noise, the limit of detection of some analytes was unacceptably high, and the LODs observed at low analyte concentration were inferior to those recorded for direct conductivity, and for stronger acids they were also inferior to pH measurement. Although baseline interferences can be eliminated, multiple parameters are involved in the system design, thus the optimisation process is challenging and is further complicated by the addition of organic solvents to the eluent. Further weaknesses of the indirect conductivity detection method is its lack of complete universality, being dependant on varying values of limiting equivalent ionic conductances, as well as analyte solubility and dissociation.

The second examined analytical technique of pH detection demonstrated higher response factors when following a suppressed system compared to following a system employing base introduction. Nevertheless, its sensitivity was inadequate and the limits of detection did not provide any advantage over suppressed conductivity detection. The conclusion from this research is that pH detection is not considered a robust option for routine work in industry, and does not comply with the need to augment the eluent with organic solvent for improved solubility of hydrophobic analytes.

In conclusion, both methods for signal enhancement demonstrated profound disadvantages, and for use as a technique for impurity analysis of ionogenic pharmaceuticals, these approaches cannot compete with more robust universal detection techniques such as evaporative light-scattering detection (ELSD), corona charged aerosol detection (CAD) and mass spectrometry (MS) as reported in Chapter 7.

3.5. References

[1] I. Berglund, P.K. Dasgupta, Anal. Chem. 64 (1992) 3007.

[2] I. Berglund, P.K. Dasgupta, J.L. Lopez, O. Nara, Anal. Chem. 65 (1993) 1192.

[3] A. Sjoegren, P.K. Dasgupta, Anal. Chem. 67 (1995) 2110.

[4] A. Sjögren, P.K. Dasgupta, Anal. Chim. Acta 384 (1999) 135.

[5] R. Al-Horr, P.K. Dasgupta, R.L. Adams, Anal. Chem. 73 (2001) 4694.

[6] A. Caliamanis, M.J. McCormick, P.D. Carpenter, J. Chromatogr. A 850 (1999) 85.

[7] A. Caliamanis, M.J. McCormick, P.D. Carpenter, J. Chromatogr. A 884 (2000) 75.

[8] S. Egashira, J. Chromatogr. 202 (1980) 37.

[9] H. Shintani, P.K. Dasgupta, Anal. Chem. 59 (1987) 802.

[10] M. Trojanowicz, M.E. Meyerhoff, Anal. Chem. 61 (1989) 787.

[11] H. Shintani, P.H. Dasgupta, Fresenius. J. Anal. Chem. 336 (1990) 38.

[12] P.R. Haddad, M.J. Shaw, G.W. Dicinoski, J. Chromatogr. A 956 (2002) 59.

[13] P. Zakaria, G.W. Dicinoski, B.K. Ng, R.A. Shellie, M. Hanna-Brown, P.R. Haddad, J. Chromatogr. A 1216 (2009) 6600.

[14] P.R. Haddad, P.E. Jackson, M.J. Shaw, J. Chromatogr. A 1000 (2003) 725.

[15] J.S. Fritz, D.T. Gjerde, Ion Chromatography, Wiley-VCH, Weinheim, 4th ed., 2009.

[16] P.R. Haddad, P.E. Jackson, Ion chromatography: principles and applications, Elsevier, Amsterdam, 1990.

[17] C. Pohl, K. Srinivasan, Y. Liu, Personal communication, Dionex Corp., Sunnyvale, CA, USA, 2010.

[18] A. Caliamanis, M.J. McCormick, P.D. Carpenter, Anal. Chem. 71 (1999) 741.

[19] P.W. Atkins, Physical Chemistry, Oxford University Press, Oxford, 4th ed., 1990.

[20] A. Caliamanis, M.J. McCormick, P.D. Carpenter, Anal. Chem. 69 (1997) 3272.

[21] M. Fotsing, B. Barbeau, M. Prevost, J. Environ. Sci. Heal. A 46 (2011) 420.

[22] R.M. Cassidy, S. Elchuk, P.K. Dasgupta, Anal. Chem. 59 (1987) 85.

[23] M. Yazdanian, K. Briggs, C. Jankovsky, A. Hawi, Pharm. Res. 21 (2004) 293.

[24] B. Beden, J.M. Leger, C. Lamy, in J.O.M. Bockris, B.E. Conway, R.E. White (Editors), Modern Aspects of Electrochemistry, Plenum Press, New York, 1992.

[25] K.C. Ong, R.A. Robinson, R.G. Bates, Anal. Chem. 36 (1964) 1971.

[26] S. Espinosa, E. Bosch, M. Roses, J. Chromatogr. A 964 (2002) 55.

[27] X. Subirats, M. Roses, E. Bosch, Sep. Purif. Rev. 36 (2007) 231.

Chapters 4-7 have been removed for copyright or proprietary reasons

1. N. Karu, G.W. Dicinoski, M. Hanna-Brown, P.R. Haddad. Determination of pharmaceutically related compounds by suppressed ion chromatography: I. Effects of organic solvent on suppressor performance. *J. Chromatogr. A.* 1218 (2011) 9037. *(Chapter 4)*

2. N. Karu, G.W. Dicinoski, M. Hanna-Brown, P.R. Haddad. Determination of pharmaceutically related compounds by suppressed ion chromatography: II. Interactions of analytes with the suppressor. *J. Chromatogr. A.* 1224 (2012) 35. *(Chapter 5)*

3. N. Karu, G.W. Dicinoski, M. Hanna-Brown, K. Srinivasan, C.A. Pohl, P.R. Haddad. Determination of pharmaceutically related compounds by suppressed ion chromatography: III. Role of electrolytic suppressor design. *J. Chromatogr. A.* 1233 (2012) 71. *(Chapter 6)*

4. N. Karu, J.P. Hutchinson, G.W. Dicinoski, M. Hanna-Brown, P.R. Haddad. Determination of pharmaceutically related compounds by suppressed ion chromatography: IV. Interfacing ion chromatography with universal detectors. (*Submitted to J. Chromatogr. A*). *(Chapter 7)*

Chapter 8

General Conclusions

The presented work has investigated the feasibility of employing ion-exchange chromatography for the determination of weakly acidic analytes in the pharmaceutical industry. The separation mechanism proved to be complementary to reversed-phase, when applied to an analyte test set comprising commonly used anionic pharmaceuticals.

The first step was to explore conductivity detection, which is the natural choice in IC. Since signal enhancement is necessary for weakly-ionised analytes, the use of a post-column reaction for this purpose was examined by *in-situ* reaction between acidic analytes and a stream of basic eluent. Then, the enhancement reaction was implemented in a flow-injection mode, comparing two different approaches for the introduction of the basic reagent. Only one of those approaches, namely base-introduction via a tee-connector, showed potential for signal enhancement, and was further examined in a complete chromatographic system. However, the obtained results did not fully meet the requirements for routine application as good signal enhancement (up to 500-fold) was recorded only for weak acids injected at high concentrations and/or injection volumes, requiring a minimum of 100 µL containing 100 µM sample. Moreover, even at such high concentrations the baseline noise levels were very high (>50 nS) resulting from pump pulsation caused by the pump used to introduce the basic reagent. Peak dispersion also occurred during mixing with the added base. The issue of pump pulsation can be solved by the utilisation of a pneumatic reagent delivery device, which would eliminate pump pulsation. In order to minimise peak dispersion, the flow-rate ratio of the suppressed eluent and the introduced base should be as high as possible (for example 0.9 mL/min eluent : 0.1 mL/min reagent), within the limitations of efficient mixing and the flow-rate and maximal pressure at the reagent delivery device. The utilisation of such a pneumatic delivery system for signal enhancement of a tailored test set of weak acid pharmaceuticals (pK_a range 4.2 to 8) will establish to a higher certainty the level of applicability of this approach.

The second detection approach investigated was pH detection, either in a standard suppressed mode or after introduction of a basic reagent. Under both conditions the pH detection did not show any advantage compared to conductivity detection in terms of signal enhancement. Another weakness of the pH detection is its lack of accuracy when organic solvents are added to the eluent, which was found necessary to minimise hydrophobic adsorption on the polymeric stationary phase and improve solubility of analytes. In addition, pH baseline drift accompanies gradient elution profiles, which are the means of generating separation selectivity for the weak ionic species under study.

Since the options for signal enhancement with conductivity detection did not provide sensitive detection for the target analytes, efforts were directed towards employment of modern universal detectors. The coupling of IC to universal detectors required a thorough examination of the coupling component – the suppressor, which is essential for de-salting the eluent prior to detection. As the commercially-available micromembrane suppressors (especially the electrolytic suppressors) were not designed to handle high concentrations of organic solvents or for use with hydrophobic analytes, several issues were identified. When assessed for the ability to neutralise complex ionic gradients containing up to 40% organic solvent, chemical suppression showed minimal noise levels, uniform low baseline and low gradient drift. Electrolytic suppression gave good performance, but with higher baseline conductivity levels and baseline drift than chemical suppression (with eluents containing methanol showing a more profound effect than those containing acetonitrile). In the case of electrolytic suppressors the observed effects were accompanied by high voltage across the suppressor, which is known to have deleterious effect on the suppressor membranes and screens. The elevated baseline was found not to be caused by incomplete suppression of the eluent, but was attributed to chemical reactions involving the organic solvents and facilitated by high electric currents and heat generation in the suppressor. When the profiles of analyte peaks were compared to those obtained before suppression, extensive band broadening (over 150%) was observed, and analyte losses of up to ~60% in the suppressor were recorded. Recovery experiments conducted in various compartments of the electrolytic suppressor showed that some of the analyte was adsorbed or precipitated in the eluent chamber, while lower quantities permeated through the

suppressor membranes into the regenerant chambers. Correlations were found between the analyte recovery rates after suppression and the eluent composition, the suppression conditions and the suppressor usage. The peak recoveries and peak broadening were also related to the physico-chemical properties of the analytes, suggesting that hydrophobic adsorption interactions had occurred in the electrolytic suppressor. Analyte loss due to these interactions was reduced to 5-20% by the addition to the eluent of high levels of organic solvents, especially acetonitrile. Chemical suppression avoided some of the analyte losses observed when using an electrolytic suppressor, but if used under the correct conditions, electrolytic suppressors gave close to equivalent performance to chemical suppressors. Another option which has not been examined is the use of longer-chain organic solvent, such as isopropanol, to eliminate interactions on the suppressor. The use of high-viscosity solvents, however, will increase the backpressure limiting their use to low concentrations (~10%). Also, the effect of such solvents on selectivity with the existing ion-exchange columns will need to be assessed.

Investigation into the mechanisms underlying the negative effects mentioned above concluded that although the electrolytic suppressor is the preferred method in terms of ease of use, a modification in its design could be beneficial for the addressed application. Three new prototype electrolytic suppressors were fabricated by Dionex Corp. for comparative assessment, incorporating high ion-exchange capacity screens and high ion-exchange capacity membranes in different thicknesses and materials. These designs were intended to minimise hydrophobic interactions of the suppressor with organic analytes and to provide higher compatibility with eluents containing acetonitrile. In comparison with the commercially-available electrolytic suppressor and also a chemical suppressor, the new designs exhibited significantly reduced interactions with the analytes, while still providing efficient suppression of a complex gradient containing organic solvent. Results of an expanded analyte test set using the best design of the three prototype suppressors, namely that comprising a new type of thicker high capacity membrane, exhibited performance which was comparable or superior to the commercially available chemical suppressors (93-99% recovery), and also showed improved peak shapes. This design was chosen for subsequent work to provide proof of concept for the coupling of IC to universal detectors.

The set of experiments coupling suppressed IC to universal detectors had two aims. The first was to compare the performance of the new suppressor design to the commercially-available chemical suppressor; and the second was to assess the suitability of each universal detector for analysis of weakly acidic pharmaceuticals after suppression of a gradient of non-volatile competing ions. The new design of the electrolytic suppressor generally showed consistent advantages over the chemical suppressor in terms of intra-day precision, limits of detection, linearity and range of linear response. Nevertheless, the results obtained with the chemical suppressor suggested that it too could also be applied to the required application. When coupled to MS and CAD, the prototype electrolytic suppressor showed precision in peak areas of between 0.4% and 2.5%, compared to the chemical suppressor which on average gave 1.5 to 3-fold higher %RSDs for the test analytes. These values were obtained after only a short set of experiments, and the robustness and reproducibility of the response should be assessed in future work. The limits of detection of the universal detectors were not greatly compromised by either of the suppression methods, yielding values below 50 ng/mL with MS, low to sub-µg/mL levels with CAD and 2-20 µg/mL with ELSD (for a 25 µL injection). For improved limits of detection, future work should explore ways to further decrease the baseline level and noise, especially on the ELSD and CAD. The prototype electrolytic suppressor also generally exhibited wider linear response ranges than the chemical suppressor when coupled to MS and CAD. The linearity of response of ten weakly anionic pharmaceuticals after suppression followed the expected behaviour for the different detectors, showcasing the feasibility of this interfacing technique for quantitative analysis. An advantage of the proposed suppressed system is the ability to separate analytes using a gradient of ionic eluent for increased selectivity instead of gradient of organic solvent as conducted in RP-HPLC. The application of a constant concentration of organic solvent prevents the non-linear response normally observed in nebulising detectors and the baseline drift following solvent gradients. Thus, separation by IC avoids the necessity to apply counter-gradients or to develop response models that would address the changes in response along the gradient. The presented IC system also provides interesting possibilities arising from combination of UV detection applied before the suppressor (thus avoiding any peak distortion induced by the suppressor), followed by suppressed conductivity of small charged species, and finally one or more of

the mass-based universal detectors. This approach can be implemented in the pharmaceutical industry for the quantification of impurities, but it would also be an attractive option in other fields, such as the food industry where non-chromophoric carbohydrates can be detected by nebulising detectors after suppressed conductivity of smaller organic and inorganic ions. The set of recommendations for operational conditions obtained for the anionic suppressors can also be employed in cation suppressors where similar effects are expected.

In conclusion, this study has led to a better understanding of micromembrane suppressors by investigating their performance and limitations with regard to eluents containing organic solvents and to their use with hydrophobic analytes. Employment of the outcomes of the suppressor investigation in suppressed IC coupled to universal detectors has proved successful, showcasing its potential as a complementary method to HPLC for various applications, especially pharmaceutical analysis.